Synopsis Report

on

DISPERSION IMAGING AND SUBSURFACE PROFILING USING PASSIVE ROADSIDE MASW SURVEY

Submitted in Partial fulfilment of the Requirements for the Degree of

Doctor of Philosophy

by

Dipjyoti Baglari

Under the guidance of

Dr. Arindam Dey

Department of Civil Engineering
Indian Institute of Technology Guwahati
Guwahati – 781039, India
October 2018

1. INTRODUCTION

In seismic surveys utilising a compressional source for surface wave generation, a large part of the generated wavefield (>2/3rd part) comprises of Rayleigh waves (Park *et al.* 1999). Rayleigh waves, while propagating through heterogeneous soil medium, exhibits dispersive characteristics i.e. different frequency component of the wave propagates with different phase velocities. Velocities of the dispersive Rayleigh waves (V_r) closely follow medium's shear wave velocity (V_s) (Xia *et al*. 1999). Therefore, by analysing the propagation characteristics of dispersive Rayleigh waves, shear wave velocity can be estimated (Park 2013). Multichannel Analysis of Surface Wave (MASW) method utilises the dispersive property of Rayleigh waves for evaluation of V_s profile of an area (Park *et al.* 1999). Shear-wave velocity has been considered as a critical engineering parameter for evaluating the dynamic characteristics of soil as it is directly related to the small-strain stiffness of soil (e.g. $G_{max} = \rho V_s^2$, where G_{max}–small strain shear modulus, ρ-density). Along with its extensive and conventional use in soil classification, it has a number of crucial geotechnical applications in the area of seismic risk studies, seismic hazard zonation, evaluation of liquefaction potential, landslide potential, slope stability, load bearing capacity, stiffness and settlement of foundation and soil (Lin *et al*. 2004, Coccia *et al*. 2011, Eker *et al.* 2012).

MASW uses multiple receivers for recording surface wave signals that increases its efficiency and accuracy over other methods such as SASW (Spectral Analysis of Surface Waves). It is a cost-efficient technique and provides the benefit of precision and swiftness in estimation of V_s profile of an area. The method is also more effective in identifying multimodal nature of surface waves. From a single receiver layout, the methodology yields 1-D shear-wave velocity profile at the middle of the receiver array (Xia *et al*. 2000). It can be easily performed in a roll along mode to cover a large range of area within a short duration and construct plots of ground stiffness in 2-D or 3-D formats through an appropriate interpolation scheme (Park *et al.* 2007).

A typical MASW survey consist of three primary parts: firstly, acquisition of raw field data of Rayleigh wavefield propagations; secondly, dispersion analysis to produce a map of phase velocity variations with frequency (known as dispersion image) and, finally, inversion analysis to obtain the V_s profile of the surveyed area. A pictorial view of various steps involved in MASW have been shown in Fig.1.The most crucial part in MASW is to extract an accurate dispersion curve from the

dispersion analysis (Stokoe *et al*. 1994, Park *et al*. 1999). This is because the accuracy of the final V_s profile primarily depends upon the accuracy of the selected dispersion curve. Hence, it is imperative to obtain a dispersion image with high resolution where dispersion curve is identified as the points of spectral maxima. The dispersion imaging process is significantly affected by various geometrical, acquisition and processing parameters (Park *et al*. 1999, Zhang *et al.* 2004).

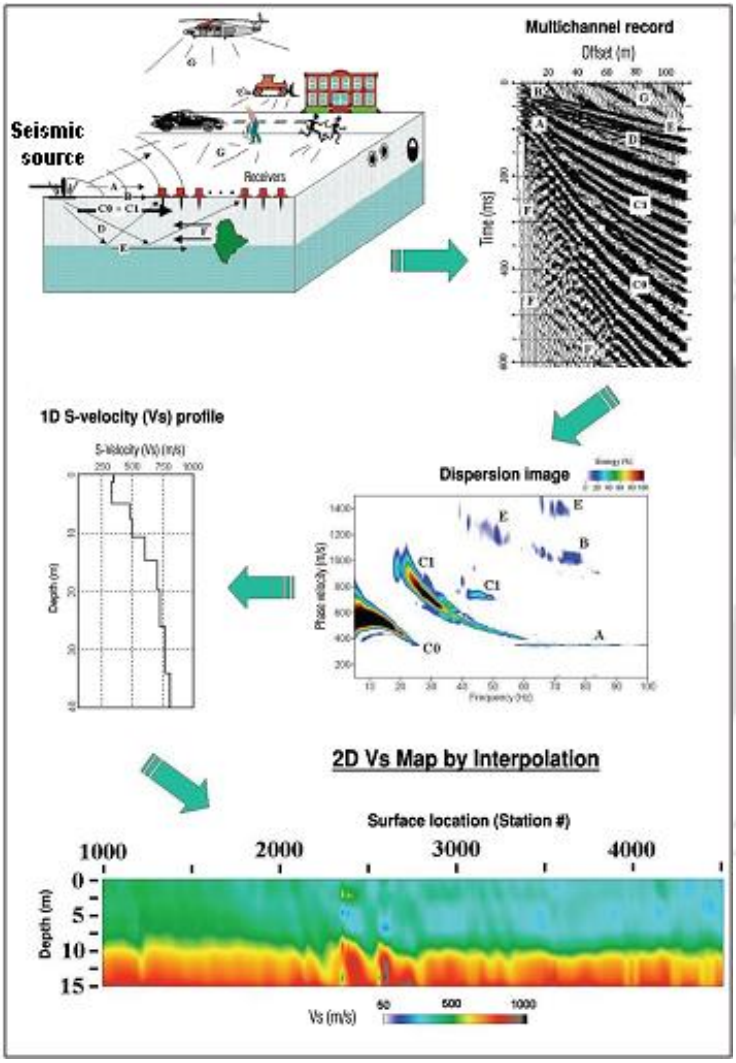

Fig. 1 Detailed procedure of MASW survey (Park *et al*.2007)

MASW survey is broadly categorised into two types based on utilisation of source of wavefield generation- Active and Passive (Park *et al.* 2007). In active survey, an impact source such as sledge hammer, weight drops etc., are utilised for the wavefield generation in the frequency band of approximately 15-50 Hz. Passive MASW uses surface waves originating from natural (e.g. tidal)

or cultural (e.g. traffic)sources, which are in the lower frequency band (longer wavelength) of approximately 5-20 Hz (Park *et al*. 2007). Therefore, passive method has the advantage of extracting subsoil information from much larger depth as compared to the active survey. However, the method requires large sized receiver arrays for effective recording of waves of smaller frequencies (Park and Miller 2008, Park *et al*. 2007, Comina *et al*. 2011). Passive MASW is again divided into two categories based on layout of receiver arrays and are called as Passive Remote and Passive Roadside. Passive remote method employs 2-D arrays such as circular, cross etc. to record natural and cultural origin wavefields. Passive roadside method utilises linear arrays to record mostly traffic-originated wavefields and is laid along the shoulder or nearby areas beside a roadway. Easier field operation and ability of deeper subsoil investigation with little compromise in accuracy makes the roadside method more practical than the remote (Park *et al*. 2007). However, very little research has been conducted on the true effectiveness and real field complicacies of roadside survey until date.

2. OBJECTIVE OF THE RESEARCH

The primary objective of this research is to critically examine various parameters controlling the resolution and quality of dispersion imaging of passive roadside data, so that robust and confident V_s profile can be obtained irrespective of site and test conditions.

3. SCOPE OF THE WORK

Following are the important scopes of the present study:

- To study the field records in terms of frequency content, energy levels and propagation characteristics, as collected in passive roadside survey, obtained from the passage of vehicles of different genre.
- To study the nature of field records in terms of spectral and contamination characteristics from sites with different traffic volumes.
- To study the effects of receiver array length and acquisition time on the collected wavefield characteristics and subsequent dispersion imaging based on the data collected from sites with different traffic volumes.
- To study the importance of scanning range of frequency and phase velocity during dispersion analysis on the resolution of dispersion imaging.

- To study the influence of different arrivals of wavefront patterns, i.e. inline-planar (IP), offline planar (OP) and offline cylindrical (OC), and their corresponding analysis schemes on the resolution of dispersion imaging.
- To study the significance of dispersion curve selection from the dispersion image, in terms of frequency band and selection density, on the accuracy and reliability of the resultant V_s profile.
- To study the influence of initial earth model on the resultant V_s profile.
- To assess the effect of source location (intra-line or outer-line) and number of sources (single or multiple) sources on the dispersion imaging.
- To identify the influence of offline distance on the usability of passive roadside MASW survey.
- To develop robust guidelines for conducting reliable passive roadside MASW survey.

4. ORGANISATION OF THE THESIS

Chapter 1 depicts the introduction to the thesis topic and the importance of V_s as a dynamic property of soil along with a brief overview of the MASW survey. **Chapter 2** presents a detailed literature survey on the various aspects related particularly to the enhancement of dispersion imaging in passive MASW survey. Subsequently, the objective and scope of the present work has been brought out. **Chapter 3** comprises the theoretical background of dispersion imaging and inversion of passive roadside MASW survey. **Chapter 4** presents details of the test sites, instrumentation and software utilized in this study. **Chapter 5** contains the detailed study of quality of raw field records from different traffic source origin in terms of its frequency and energy content and its impact on dispersion imaging. **Chapter 6** describes the influence of acquisition parameters, namely the length of receiver array and acquisition time, on dispersion imaging for sites carrying different traffic volume. **Chapter 7** presents the influence of various processing parameters such as scanning range of frequency and phase velocity, searching quadrants, processing scheme and vertical stacking on the resolution of dispersion image. **Chapter 8** presents the effect of dispersion curve selection in terms of range of selection and density of points on the accuracy and reliability of resultant V_s profile. **Chapter 9** describes the significance of source location and offline distance of receiver array on the resolution of dispersion imaging. **Chapter 10** presents the summary and

conclusions drawn from the present study, as well as highlighting the limitations of the present research and scope of future works.

5. BASICS OF PASSIVE MASW SURVEY AND ANALYSIS

As previously mentioned, dispersion analysis is the most critical stage in MASW technique. The ground roll data acquired from the field survey is normally represented as the time-domain displacement data. In phase shift method of dispersion analysis (Park *et al*. 1998), each time-domain record is transformed into frequency-domain by applying Fast Fourier Transformation. The transformation separates different frequency component of the wavefield. Thereafter, energy (or amplitudes) of the wavefield is estimated by a summation over the traces, for each frequency component in a scanning range of phase velocity after applying a necessary phase shift for each trace. The appropriate phase velocity is the one for which summed energy is maximum at a particular frequency. This summation process is carried out over different frequency components and finally frequency v/s phase velocity image is constructed by stacking of each energy-phase velocity space. Thus, based on the final image, commonly called as dispersion image, the dispersion curve is extracted by extracting the points of highest energy (characterized by a colour map on the dispersion image in currently used software platforms). Normally, larger traces makes thinner energy band with sharp resolution of the energy band.

Dispersion imaging in passive MASW is more complicated than active survey attributed to unknown number and locations of source and direction of incoming signals. Park *et al*. (2004) modified the phase shift method for active MASW survey to be applicable for passive method. In the modification, a parameter for direction of incoming wavelength, i.e. azimuth, was considered in addition to frequency and phase velocity. For each frequency component, energy for a scanning phase velocity is calculated by assuming an azimuth. The calculation is carried over a scanning range of phase velocity much like the case for 1-D analysis and then over a scanning range of the azimuth (e.g. 0-360 degrees). Finally, all the energy in the phase velocity-azimuth space is stacked along the azimuth axis that collapses the azimuth space to leave only phase velocity space. The process is repeated at different frequencies to produce the final image in phase velocity-frequency space. The dispersion-imaging scheme for passive roadside survey (Park and Miller 2008) is similar to that used in passive remote survey. In passive roadside survey, the wavefield arrival in

the receiver array can be of three types depending upon position and proximity of the source producing the wavefield- Inline Plane (IP), Offline Plane (OP) and Offline Cylindrical (OC). When the source is in the same alignment and at a large distance from the receiver array, the wave arrival is mostly of IP type. The OP type of wave will be recorded if the source is at a large distance and offline to the receiver array. If the source is situated very close and offline to the receiver array, the wave arrival will be OC type. The modified scheme for roadside survey takes account of the possible distance of the source from the receiver array and thus accounts for the three types of wave arrival.

6. FIELD SET UP AND METHODOLOGY

In the current work, three site locations, inside and around IIT Guwahati campus have been selected for an extensive passive roadside experimentation (Fig.2).The three test sites are:

- **Site 1**: Inside IIT Guwahati campus in the roadside near the cricket field between SAC and hostel Siang (26º1127"N, 91º4145"E).
- **Site 2**: A part of the road stretch from IIT Guwahati to Amingaon market (26º1056"N, 91^{0}4135"E).
- **Site 3**: Beside National Highway (NH) No. 31, over a stretch between Jalukbari to Baihata Chariali route (26º1238"N, 91º4122"E).

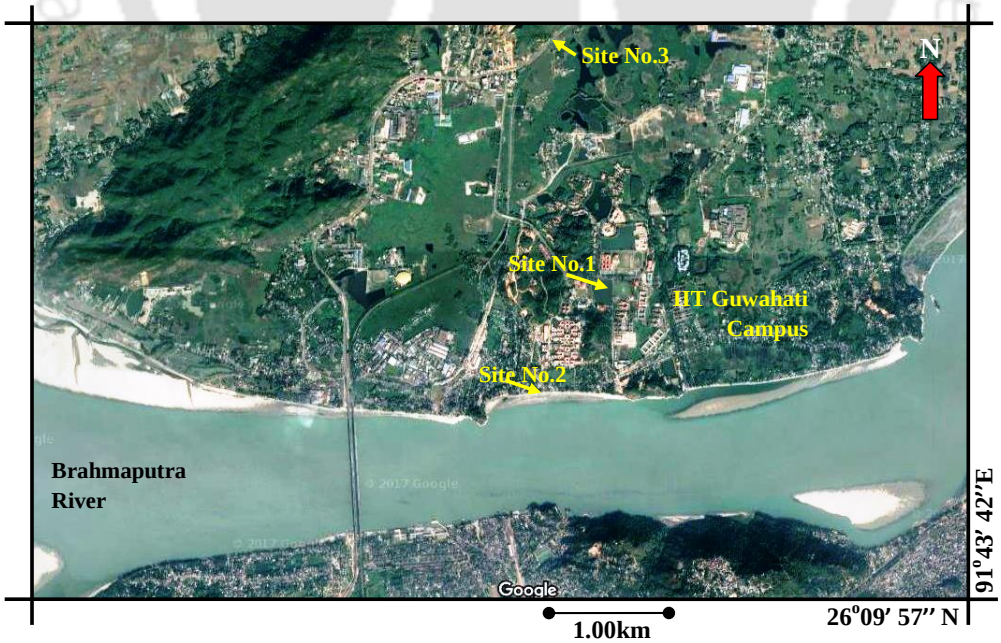

Fig. 2 Map showing positions of the Sites 1, 2 and 3 in and around IIT Guwahati campus

All the sites comprise different volumes of traffic: light at Site 1 (Less than 50 commercial vehicles per day), medium at Site 2 (50-150 commercial vehicles per day) and heavy at Site 3 (more than 150 commercial vehicles per day). The sites were selected based on two primary criteria. Firstly, the road beside the site should have a straight alignment as far as possible (23 m to 100m) so that a linear receiver array can be placed with a constant offline distance. Secondly, there should not be any intersectional major road or other structures that could hinder laying of the receiver array as well as could possibly produce traffic waves from unwanted directions. The primary field parameters such as receiver numbers, receiver array type and size adopted during the survey at the three sites have been shown in Table 1.

Table 1 Details of the receiver array type and dimension utilized at different sites

Site	Receiver Numbers	Receiver array shape	Dimension or Length of receiver array (m)		
			Passive Roadside	Active	Passive Remote
1	12, 24	Linear for roadside/active Circular for remote	23, 46, 69	11, 23, 46, 69	18 m dia.
2	24	All linear	23, 46, 92	46	----------
3	24	All linear	46, 92	46, 92	----------

Table 2 Details of the acquisition time used at different sites and different modes of survey

Site	Survey type	Acquisition time (s)
1	Roadside	0.7 - 218
	Active	1
2	Roadside and remote	10.8
	Active	1
3	Roadside	0.7 - 218
	Active	1

Another recording parameter that is influential during passive MASW survey is the recording or acquisition time. For passive survey (both remote and roadside), acquisition time is a site-specific parameter and needed to be modified (augmented or reduced), depending on site conditions of traffic volume and passive source existence. According to normally adopted axiom, there should

be at least one occurrence of movement of a vehicle near the surveyed area during the acquisition time. Details of various ranges of acquisition time adopted in this work for various modes of MASW survey at the three sites has been presented in Table 2.

All the raw field data obtained from the three sites with different mode of survey have been processed using a commercialized software platform "Surfseis". The working principle of the software is based on the dispersion imaging process proposed by Park *et al.* (1998) for active, and Park and Miller (2008) for passive roadside survey.

7. CRITICAL ANALYSIS OF RAW FIELD RECORDS

In MASW survey, a good quality data is considered to be the one in which surface wave event is the most significant and possesses a high signal to noise ratio (SNR). On the other hand, a bad quality signal is the one that is highly contaminated by various noises, and possesses poor SNR. Noise in MASW survey implies body waves, airwaves, backscattered waves and higher mode surface waves. Primarily, fundamental mode surface waves are considered as signal during dispersion curve analysis ignoring all other as 'noise'. Primary factors affecting the characteristics of recorded wavefield in roadside survey are the weight and speed of vehicles, number of vehicles crossing the receiver array during recording, and source characteristics upon the road surface such as its size and their positions.

7.1 Study of raw field records from various sources at Site 1

7.1.1 Study of raw field records from zero traffic and from a single vehicle

At first, tests have been conducted to study the influence of the presence and absence of vehicular movement on the recording of wavefield data. The existence of ambient noises, other than the traffic, which may be recorded during actual roadside recording, has been also checked. It has been observed in Fig. 3a and 3c that even with the most silent traffic environment, some nominal microtremors have been recorded and that has also been manifested in the form of the minor energy accumulation in the lower frequency band (<12 Hz) on the dispersion image shown in Fig. 5a. In Fig. 3b, a typical field record has been shown when one car weighing around 1000 kg passed through the receiver array at a speed of approximately 40 kmph. Wavefields created by the vehicle (Fig. 3d) are nearly of identical energy magnitudes and no noticeable strong surface event occurred

during the recording manifesting absence of major surface sources. These wavefields were recorded from the vibrations generated during movement of the vehicle on the rough surface of the bituminous pavement generating mini surface events recordable only when vehicle reaches close to the receiver array. From the frequency spectrum of the two records (Fig.4a and 4b), very weak signals in case of the first record and slightly stronger signals of the second record can be observed. Dispersion image in case of the second record (Fig.5b) shows a marginal improvement in the lower frequency band attributed to the relatively stronger wavefield from the vehicular movement.

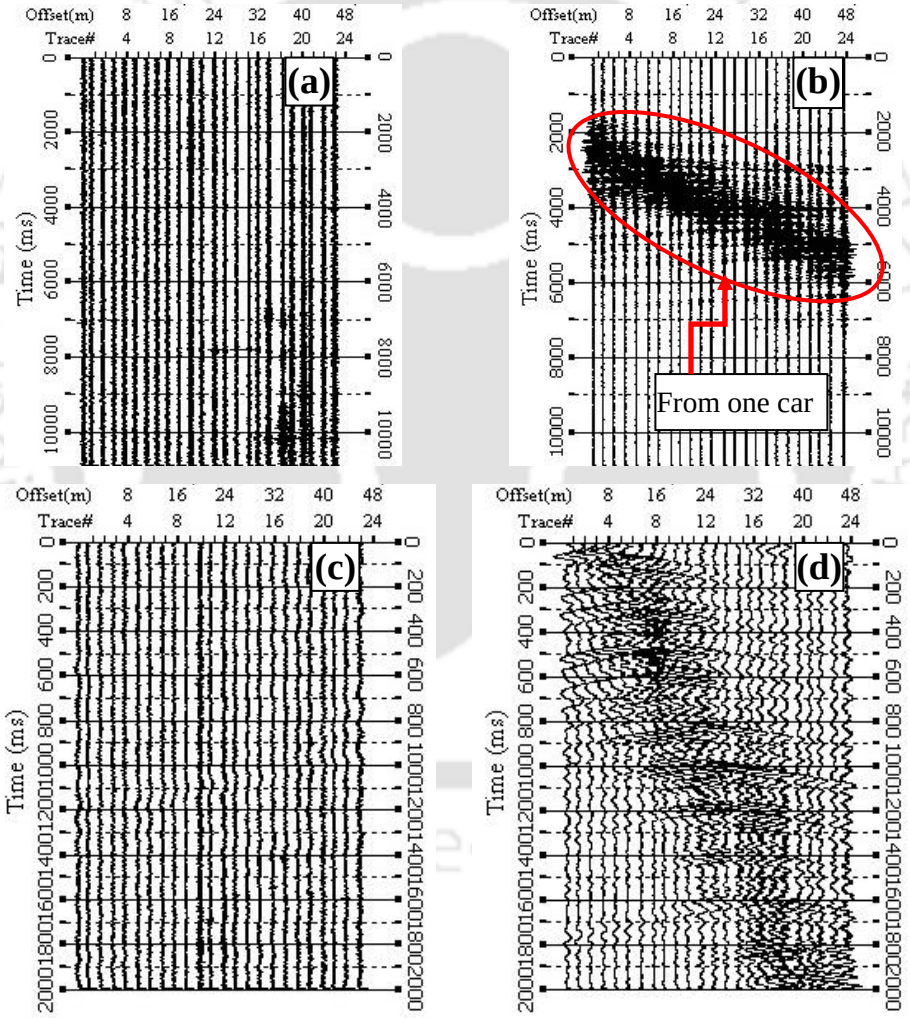

Fig. 3 Raw field recordfrom(a) zero traffic **(**b) one car movement(c) enlarged portion of record 'a' between 0-2000 ms (d) enlarged portion of record 'b' between 3000-5000 ms

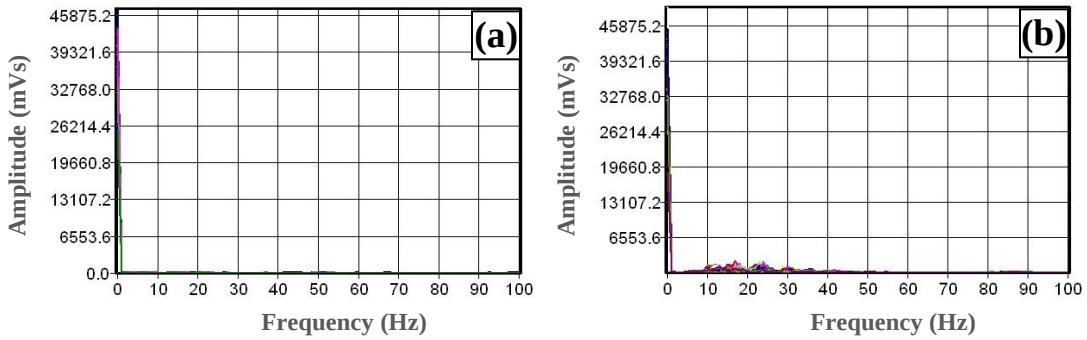

Fig. 4 Frequency spectrum of field record with (a) zero traffic (b) one vehicle movement

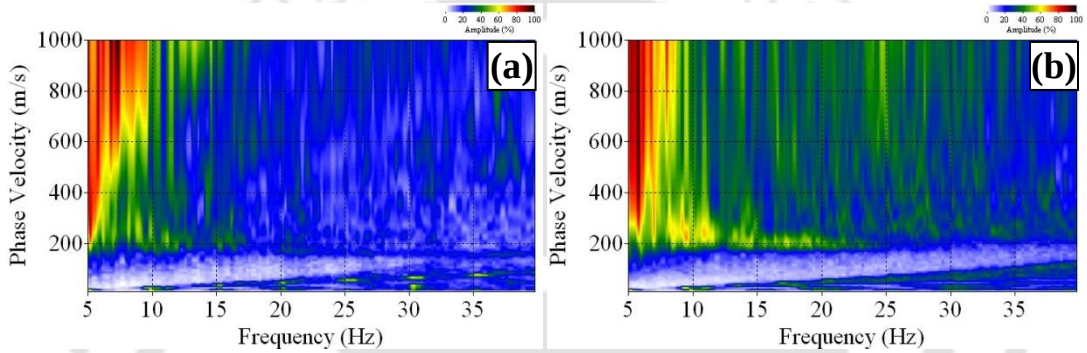

Fig. 5 Dipsersion images from field record with (a) zero traffic (b) one vehicle movement

7.1.2 Study of raw field records from large weight vehicles

The record shown in Fig.6a was collected during passage of a school bus of weight approximately 10000 kg by the receiver array. The enlarged view of the record (Fig. 6c) shows similar nature of wavefields as observed in the previous section with a light vehicle movement. However, movement of the heavy bus created wavefields with much higher energy that has been manifested in the frequency spectrum of the record(Fig.7a).Figure 6b shows a field record acquired during passage of a heavy road roller of approximately same weight of the bus (i.e. 10000 kg) through the receiver array. Significant wavefield energy has been recorded attributed to the severe vibrations caused by the heavy road roller during its movement. In the enlarged view of the record (Fig. 6d), all the wavefields have been observed to be very densely spaced and no proper dispersion nature can be spotted in the time domain data.

From the frequency spectrum of the records (Fig. 7a and 7b), energy content of the wavefields from the passage of road roller has been found to be significantly higher than that was originated from the motion of the bus. Further, the frequency spectrum of the record is much wider in the road roller motion in the range of 10 to 50 Hz. Dispersion images for both the records have shown significant energy accumulation attributed to the large energy content in their raw data. Dispersion image in case of the field data originated from bus has shown better resolution (Fig. 8a and 8b), attributed to the quality of raw data mentioned above.

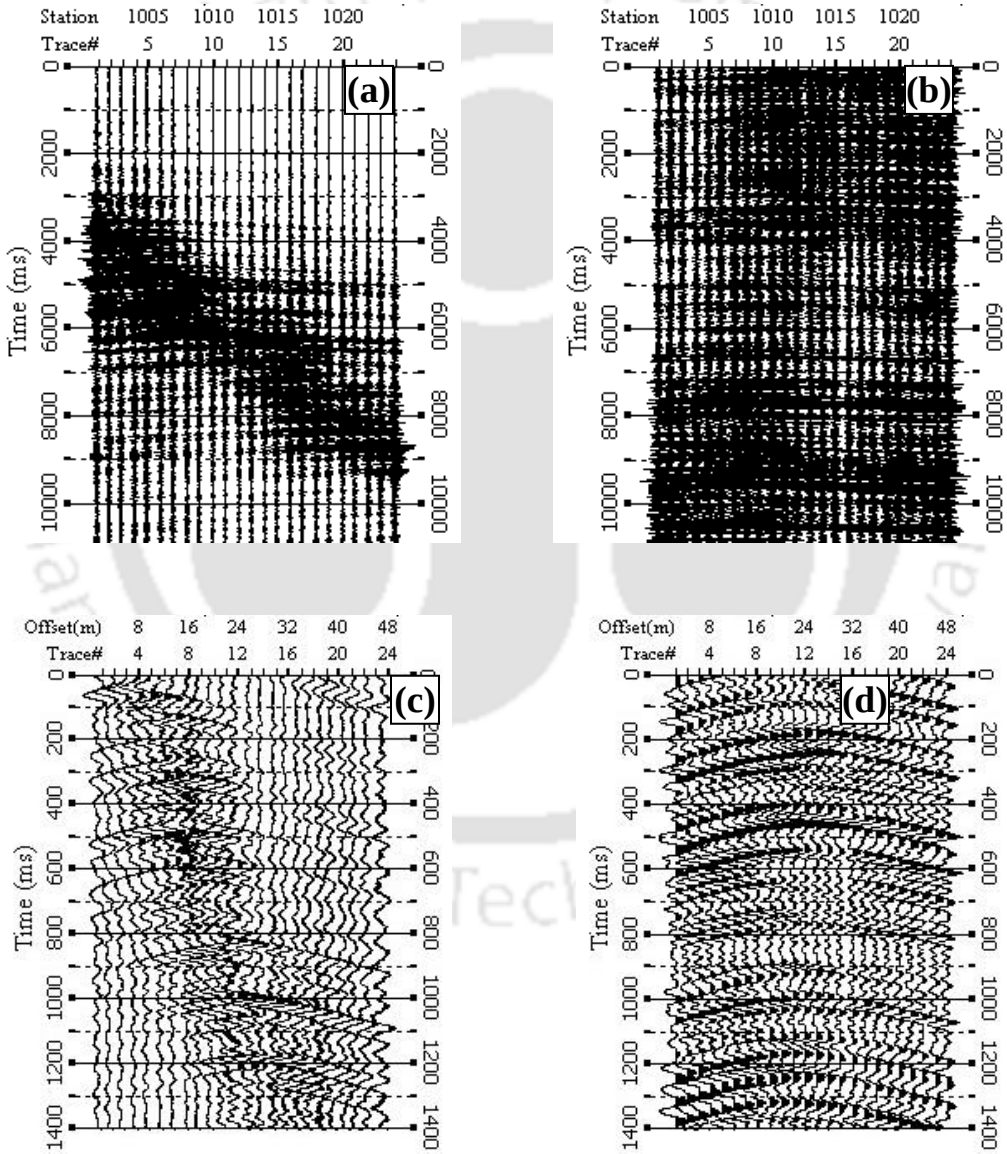

Fig. 6 Raw field record (a) acquired during passage of bus (b) acquired during passage of a heavy road roller (c) enlarged view of record 'a' (d) enlarged view of record 'b'

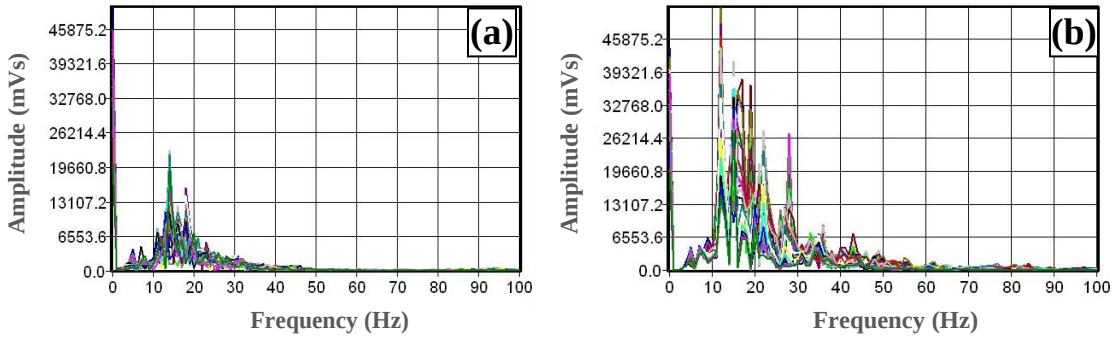

Fig. 7 Frequency spectrum (a) after passage of a bus (b) after passage of a heavy road roller

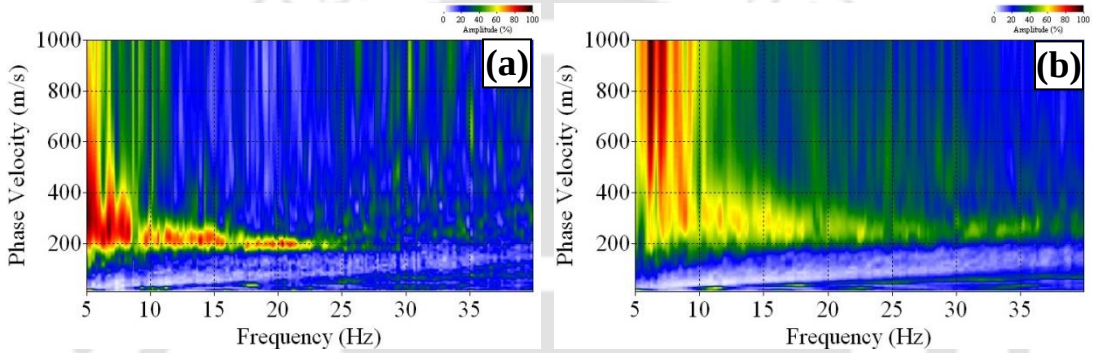

Fig. 8 Dispersion images (a) From record 'Fig. 9a' (b) From record 'Fig. 9b'

7.1.3 Study of raw field records from multiple vehicle movements

Figure 9a shows a raw field record when two cars, weighing approximately 1000 kg each, crossed the receiver array during data acquisition. Two bunches of wavefields have been observed- first one travelling from left to right in the time frame of 2000 to 6000 ms and the second one travelling from right to left in the time frame of 7000 to 10400 ms, manifesting the opposite motion of the cars. Thus, the two wavefields have been recorded without being superimposed onto each other. On the other hand, in the record shown in Fig. 9b, two vehicles coming from opposite directions have crossed each other during recording of the signal. Wavefields from both the vehicles started propagating into the array at 4000 ms from both the sides and superimposed with each other between 6000 to 8000 ms period. Dispersion images from the two records provides only a meagre information about dispersive behaviour of surface waves (Fig. 10a and 10b);only some minor energy accumulations have been observed in the two images without any regular trends. Although it was expected that the record without wave superimposition to contribute more in achieving a

better quality dispersion image, the difference in the resolution between the two dispersion images due to the superimposition of the wavefields could not be distinguished from the two images. Again, on vertically staking 10 numbers of dispersion images from both the types of field records, with and without contamination, the final dispersion image is found to be having better resolution with a continuous energy trend, implying that vertical stacking can substantially negate the effect of contaminated records (Fig. 10c).

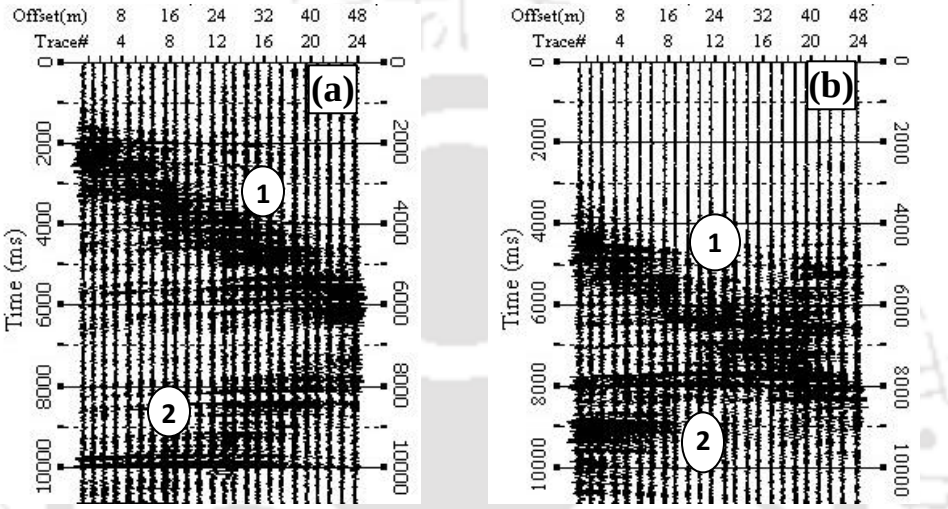

Fig. 9 Raw field record during motion of two cars (a) without superimposition of wavefields (b) with superimposition of wavefields

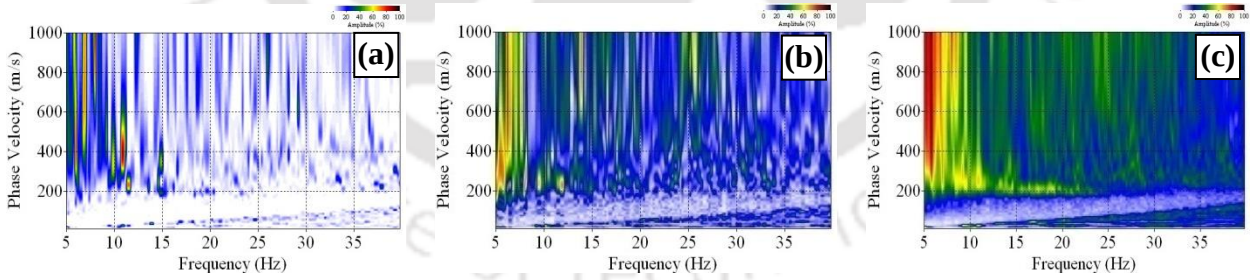

Fig. 10 Dispersion images (a) From record '9a' (b) From record '9b' (c) by stacking 10 dispersion images from raw field records of both types

7.1.4 Study of raw field records from a strong source of wavefield generation

Figure 12 shows a field record of a passive roadside survey, conducted at Site1 with a known position of a strong source (a GI rod at 20 m source offset shown in Fig. 11) of surface wave generation. Between 2000 to 4000 ms, two narrowly spaced major wavefields with a linear arrival

pattern have been observed. These two wavefields were created by the front and rear axle wheels of the vehicle while passing over the source, and the gap between the two wavefields manifest the amount of time required for the two set of wheels to pass over the source one after the other.

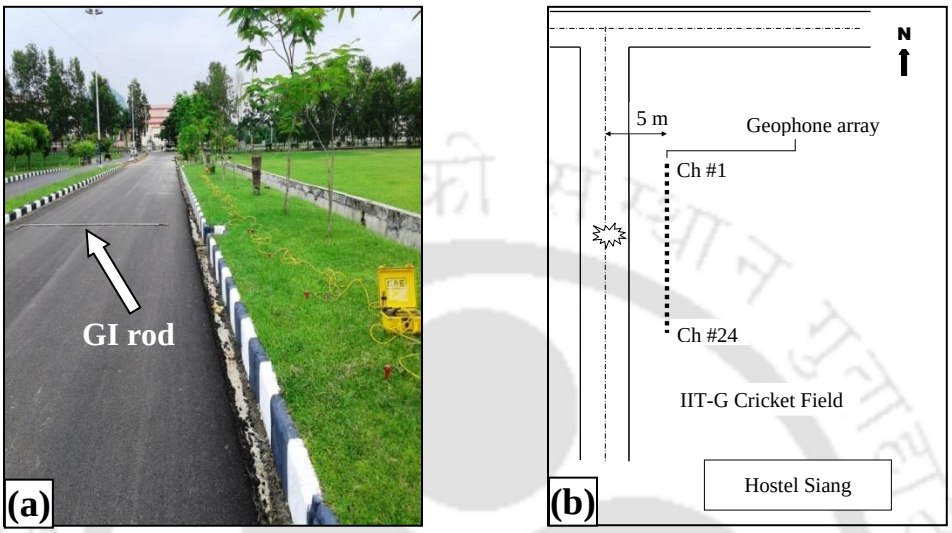

Fig. 11 (a) Pictorial view of Site 1 with placed GI rod as source (b) Schematic of field set up at Site 1

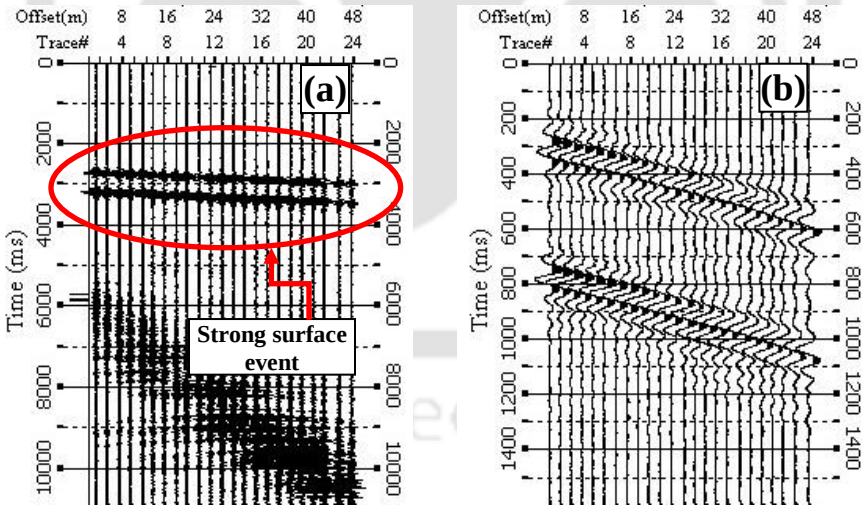

Fig. 12 Field record (a) at 10.8 s (b) enlarged view of the record between 2400-4000 ms

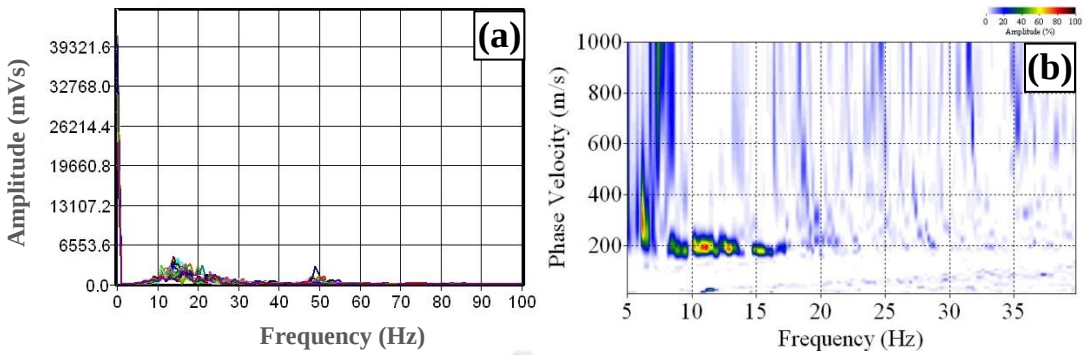

Fig. 13 (a) Frequency spectra of field record with major surface event (b) Dispersion image from the record

The dominant frequency band in the record has been found to be 10 to 30 Hz (Fig. 13a). The resultant dispersion image (Fig. 13b) comprises better resolution but not sufficient attributed to the field record generated by the vehicle of smaller weight. Hence, to develop a dispersion image with better resolution, either a major impact by heavier vehicle is required, or multiple number of vertical stacking should be utilized.

7.2 Study of raw field records from Site 2

The pictorial and schematic view of Site 2 has been shown in Fig. 14. Two typical field records collected from the site with a 46 m receiver array have been shown in Fig. 15. During the recording of the first record, at least two vehicles crossed the receiver array that is manifested by the two major wavefield (1 and 2 in Fig. 15a) regions. However, no major surface event was created by the vehicles during the recording. In the second record (Fig. 15b),one major surface event was created attributed to the passing vehicle hitting a pothole, or other such source, in the early part of the recording time in between 0 to 400 ms, due to which higher energy content of the wavefield have been observed (Fig. 16). Attributed to an average traffic flow at the site (50-150 commercial vehicles per day), obtaining records of marginal contamination and superposition of wavefield was possible.

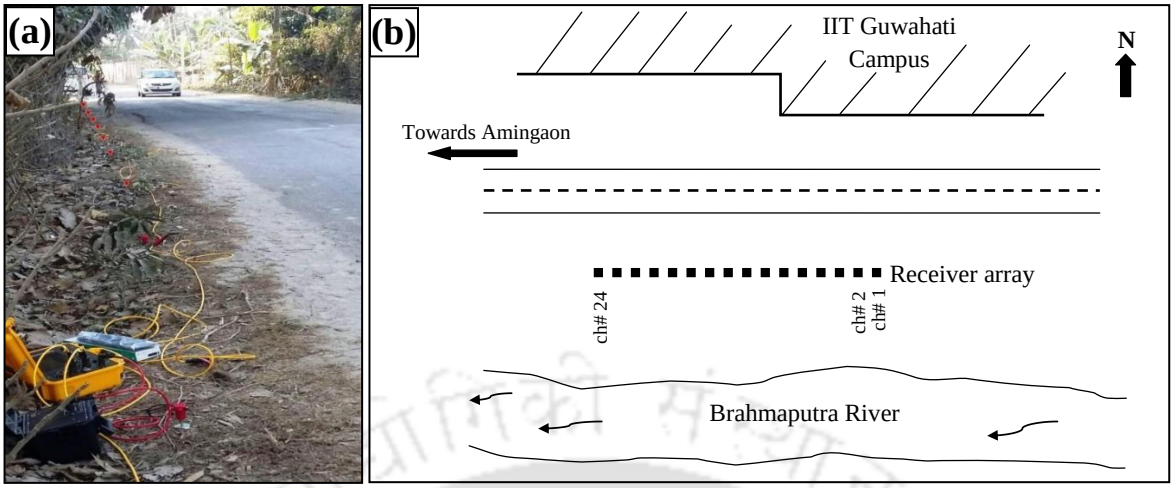

Fig. 14 (a) Pictorial view of Site 2 (b) Schematic of field set up Site 2

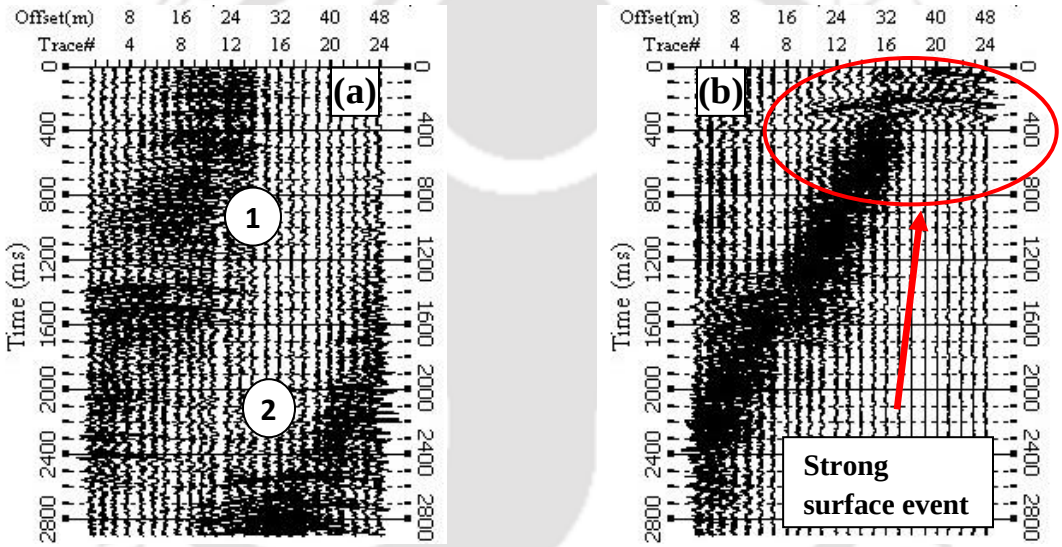

Fig. 15 Field record (a) with no significant surface event (b) with a significant surface event

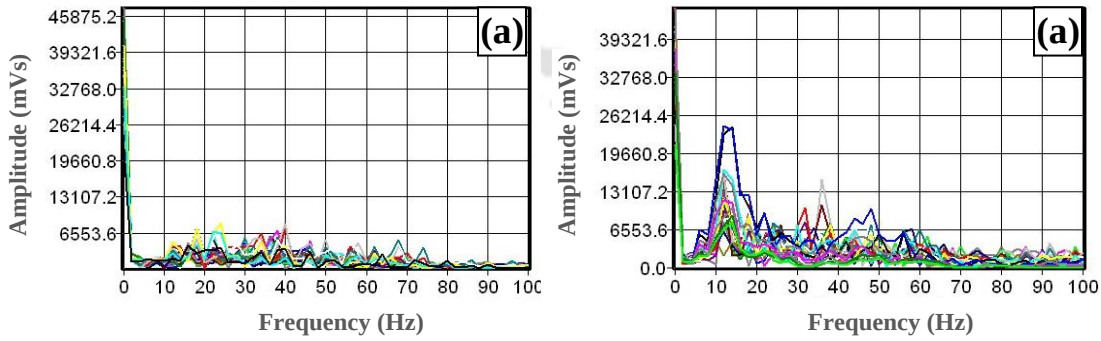

Fig. 16 Frequency spectrum (a) of the record with no significant surface event (b) of the record with a significant surface event

7.3 Study of raw field records from Site 3

Figure 18 shows two field records obtained from Site 3 with a 46 m receiver array (Pictorial and schematic view shown in Fig. 17). The first record (Fig. 18a) comprises fair uninterrupted wavefield with many events reaching to the farthest of receivers. In the second record (Fig. 18b), many events had occurred at the same time and thus superimposed and contaminated each other despite limiting the recording in a short time of 1.4 s. Here, waves generated from vehicular movements from both directions arrived at the receiver array and suffered superimposition nearly at the middle of the array. From the frequency spectrum of the record (Fig. 19), the dominating frequency band of the record has been found to be in between 10-30 Hz. The peak amplitude of the recorded wavefield is very high attributed to the movement of heavy vehicles with very high speed (nearly double than that obtained at Site 2 in the previous section).

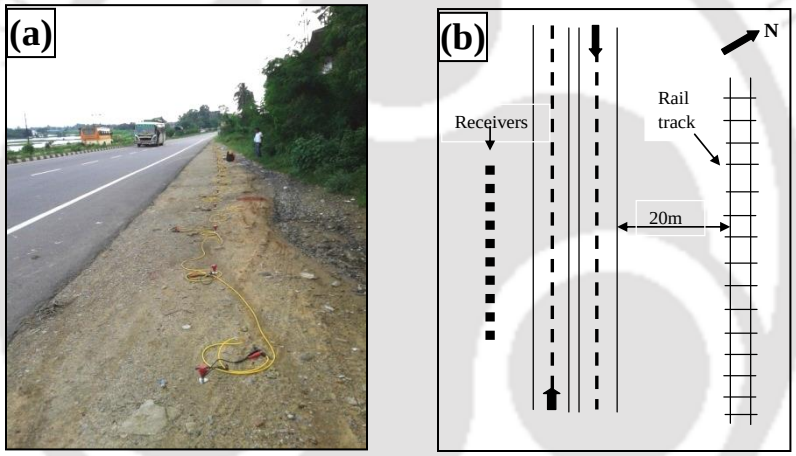

Fig. 17 (a) Pictorial view of Site 3 (b) Schematic of field set up at Site 3

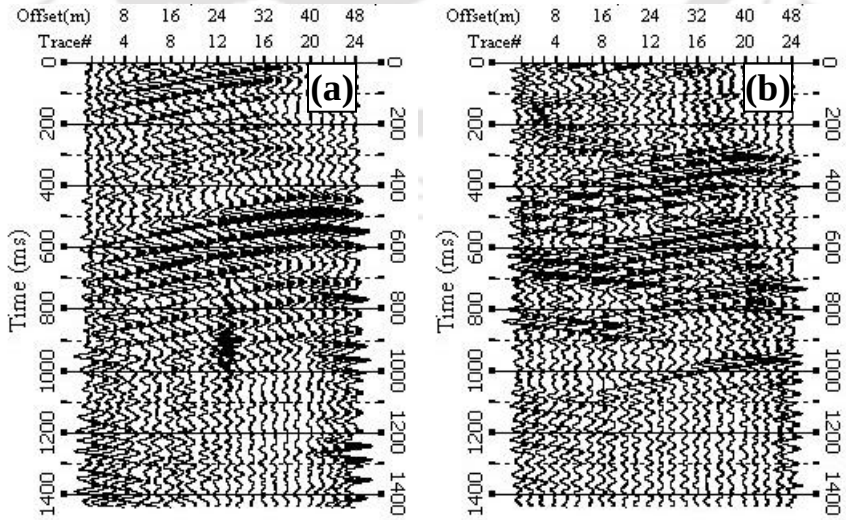

Fig. 18 Field record (a) without siginifant contamination (b) with severe contamination

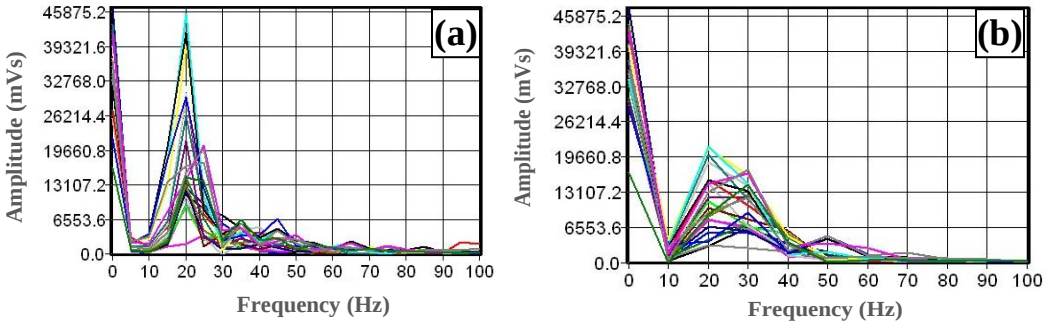

Fig. 19 Frequency spectrum of the record (a) without siginifant contamination (b) with severe contamination

8. SIGNIFICANCE OF DATA ACQUISITION PARAMETERS ON DISPERSION IMAGING

8.1 Influence of Length of Receiver Array

Generally**,** a longer receiver array is considered to give better results in terms of resolution of dispersion image (Xia *et al*. 2004). However, using a long receiver array may not be always feasible especially in congested urban areas. Moreover, it is also highly laborious to lay a longer array repetitively during field survey. Nevertheless, applicability of shorter receiver array in roadside survey has not been experimentally explored until date.

8.1.1 Study in Site 1

To critically examine the influence of length of receiver array (or inter-receiver spacing) on the resolution of dispersion image, an extensive experimentation programme has been conducted at Site 1. Figure 20 shows dispersion images obtained from array lengths of 23 m, 46 m and 69 m, respectively. A significant enhancement in the resolution of dispersion image with increase in the array length has been observed. The resolution of dispersion image obtained from the field record of 23 m receiver array (Fig. 20a) is significantly poor particularly in lower frequency band. It comprises a thick energy band wherein it is difficult to precisely locate the points of dispersion curve on the image. This is attributed to the fact that smaller receiver array poorly samples low frequency components of the wavefield and aliasing of the signals appear in low frequency band. The lowest frequency at which phase velocity can be approximately selected is 15 Hz. With increasing in the receiver array lengths, range of lowest frequency for phase velocity estimation

augments. With array length of 46 m and 69 m, the range of lowest frequency achieved were almost 9 Hz and 6 Hz respectively that will assist in deeper subsoil investigation.

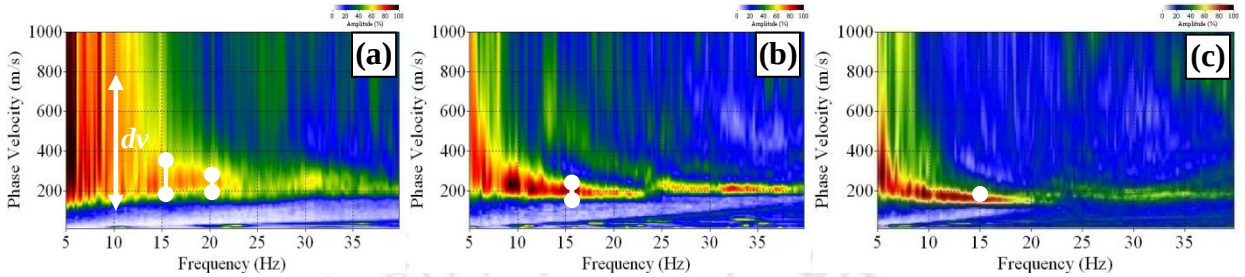

Fig. 20 Dispersion images from array lengths: (a) 23 m (b) 46 m (c) 69 m.

According to the theory of Zhang *et al.* (2004), resolution of the dispersion image can be defined as the resolvable capabilities both along the velocity and frequency axis. On a dispersion image narrower the energy bandwidth, easier and accurate is the extraction of dispersion curve. Hence, based on the width of the energy band of the dispersion image, resolution of dispersion image can be quantified. On the dispersion image shown in Fig. 20, the width of the energy band along the velocity axis is defined by a term *dv*. The value of *dv* at the frequency coordinate of 15 Hz is nearly 200 m/s. Again, in Fig. 20c, the value of *dv* at 15 Hz is mere 25 m/s. Hence, resolution of the dispersion image from a 69m receiver array is better than the image of 23 m array. The values of *dv* are much larger in lower frequency band indicating greater possibility of errors in phase velocity computation in the same. This will affect the accuracy of deeper layer information of a finally inverted V_s profile.

Table 3 Values of *dv* at different frequency coordinate for different receiver array lengths

Array length	Value of *dv*(m/s) at frequency coordinate of			Quality of dispersion image
	10Hz	15Hz	20Hz	
23 m	Undefined	200	80	Poor
46 m	80	50	30	Fair
69 m	40	20	10	Good

V_s profiles obtained from different receiver lengths have been shown in Fig. 21. Short receiver arrays, such as 23 m array, yielded poor resolution in lower frequency band of the dispersion image and attributed to which dispersion curve extraction was not possible from the lower frequency

bands. This finally resulted in attaining lesser investigation depth compared to *Vs* profile obtained from longer array lengths. With increasing in the length of the receiver array, the depth of investigation significantly increases, attributed to the effective extraction of dispersion curve from the dispersion image of enhanced resolution, particularly in the lower frequency band. With 23 m, 46 m and 69 m, the depth of investigations achieved are approximately 6 m, 15 m and 18 m respectively.

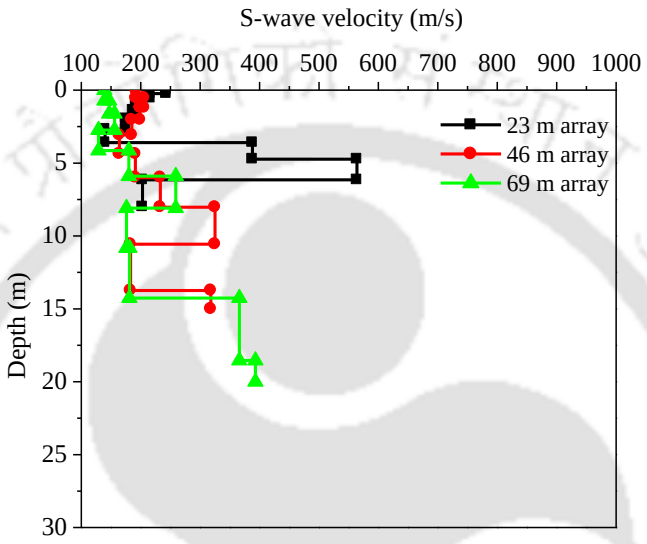

Fig. 21 Shear-wave velocity profile obtained with different lengths of receiver arrays

Table 4 represents the co-ordinates of the first point of the dispersion curve selection in terms of frequency (lowest), phase velocity and wavelength for the three receiver arrays along with attainable depth of investigation. The longest wavelength that could be collected from the receiver arrays of length 69 m, 46 m and 23 m before aliasing are 50.4 m, 41.6 m and 17.3 m respectively. Thus, the average ratio of longest recordable wavelength to receiver array length is approximately 0.8. Therefore, it can be concluded that with a receiver array of length X, the longest wavelength that can be sampled is 0.8X. The depths of investigation obtained from the three cases are 17.7 m, 14.6 m, 6.2 m respectively. Therefore, the average ratio of investigation depth to the longest wavelength recorded without aliasing is approximately 0.35-0.4. In other words, if the longest wavelength recorded by an array is Z, then the attainable maximum investigation depth is 0.4Z through a passive roadside MASW survey.

Table 4 Comparison between receiver array length, longest wavelength recorded and depth of investigation

Receiver array length (m)	Co-ordinate of the first point of dispersion curve			Depth of investigation (m)	Ratio of longest wavelength to array length	Ratio of depth of investigation to longest wavelength
	Frequency (Hz)	Phase velocity (m/s)	Wave-length (m)			
69	5.5	288	50.4	17.7	0.73	0.35
46	6.5	272	41.6	14.6	0.90	0.35
23	12.6	218	17.3	6.2	0.75	0.36

8.1.2 Study in Site 2

Tests have been conducted at Site 2 with receiver array lengths of 23 m, 46 m and 92 m respectively. All arrays have been placed at an offline distance of 3.5 m from the centre of the road. The result from the experimental work shows similar characteristics with results as obtained from Site 1. The dispersion image obtained from 23 m receiver array has high-energy content, but with indistinct dispersion trends (Fig. 22a). It comprises a thick energy band similar to the one obtained in Site 1 with same array length. With increase in the array length, the undesirable energy accumulation on the dispersion image could be avoided resulting in a more distinguishable, clearer and thinner dispersion band as shown in Fig. 22b and 22c, representing dispersion images from 46 m and 92 m array, respectively. The records from 92 m receiver array have produced the best dispersion image with a thinner and distinct fundamental mode energy band in a large frequency band of 5 to 20 Hz.

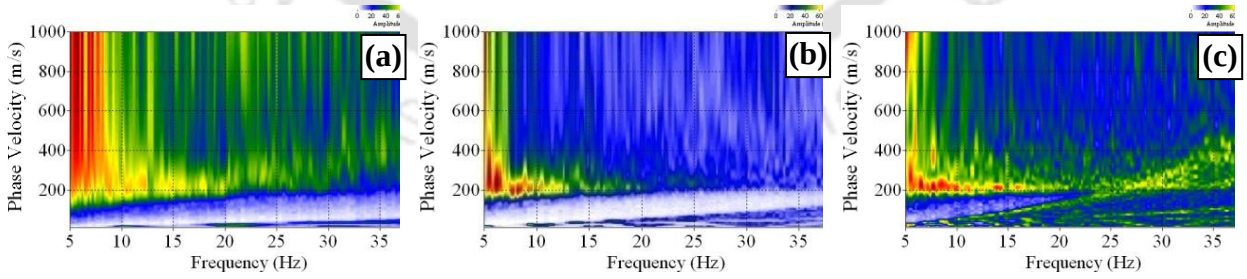

Fig. 22 Dispersion images obtained from array length of (a) 23 m (b) 46 m (c) 92 m

Validation of the study with active MASW survey (Site 2):

To validate the results from roadside survey, active test with 46 m receiver array and 6 m source offset were performed at the site. The resultant dispersion image (Fig. 23a) has nearly similar

energy trend as observed in the dispersion image from roadside survey with same array length (Fig. 22b). The corresponding dispersion curve extraction has been shown in Fig. 23b which has been done keeping highest SNR value close to the value of 1 (or 100%) at every selection of point. Minor deviations in V_s values at the uppermost 2 m layer between the two profiles have been observed (Fig. 24a). The most significant deviation between the two V_s profiles can be observed in the segment between 7 to 10 m. Figure 24b shows percentage variation of the two V_s profile obtained from the roadside and active survey. The highest deviation between the two profiles is nearly 100%. However, in all other depth range the differences in V_s values are minimal and portrayed by the closeness of the profile towards the zero difference line. In both V_s profiles, top soil layers has shown high V_s values that signifies the higher stiffness of the top layer of the road. After 3-4 m depth, V_s significantly decreases up to a depth of 7-10 m, manifesting loose soil underlying the base layer of the road. These characteristic of the subsoil were expected and seems geologically suiting for the site. Importantly, the highest wavelength of the wavefield obtained during dispersion curve selection and corresponding depth of investigation from passive roadside survey obtained are46.91 m and 15.5m respectively. Thus, ratio between depths of investigation to the highest wavelength is 0.31. However, with increase in the receiver array length to 92 m, the longest wavelength recorded was found to be nearly same with 46 m array length.

8.1.3 Study in Site 3

As the number of vehicles passing through Site 3 is large, the surface wavefield produced from one vehicle from a surface source possesses greater possibility to be contaminated from another source created by another vehicle. Hence, shorter arrays are expected to have greater possibility of recording cleaner records before being contaminated from other incoming waves. It has been observed that the shorter array of 46 m have recorded comparatively cleaner record compared to a 96 m array (Fig. 25). Expectedly, the resolution of dispersion image obtained from 46 m receiver array has been found to be better than the 96 m array (Fig. 26a and 26b). It was observed that the dominant frequency band of the records lies between 15-30 Hz.

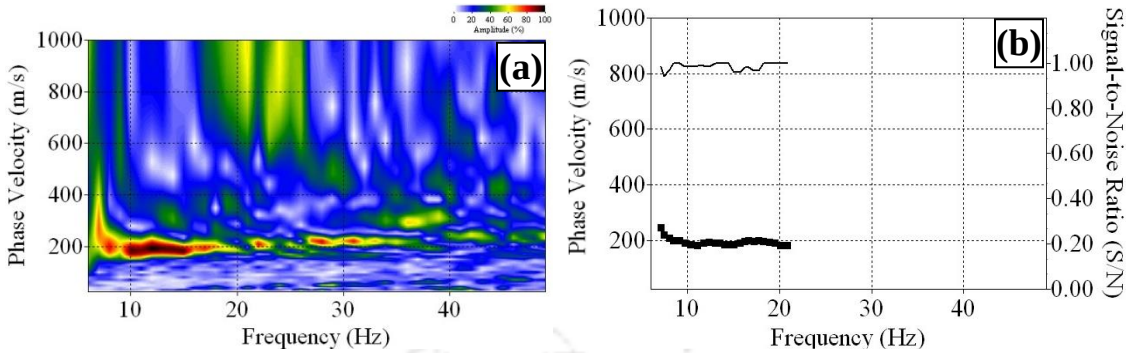

Fig. 23 (a) Dispersion image obtained at Site 2 from active test (b) dispersion curve extracted from dispersion image of active test.

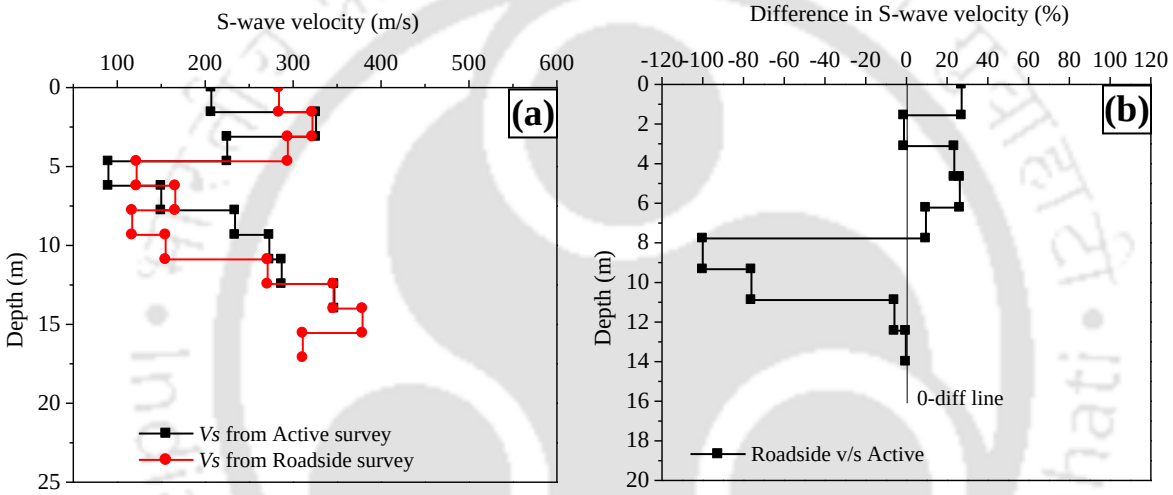

Fig. 24 (a) Comparison of S-wave velocity obtained from passive roadside and active survey at Site 2 (b) Percentage difference of S-wave velocity between passive roadside and active

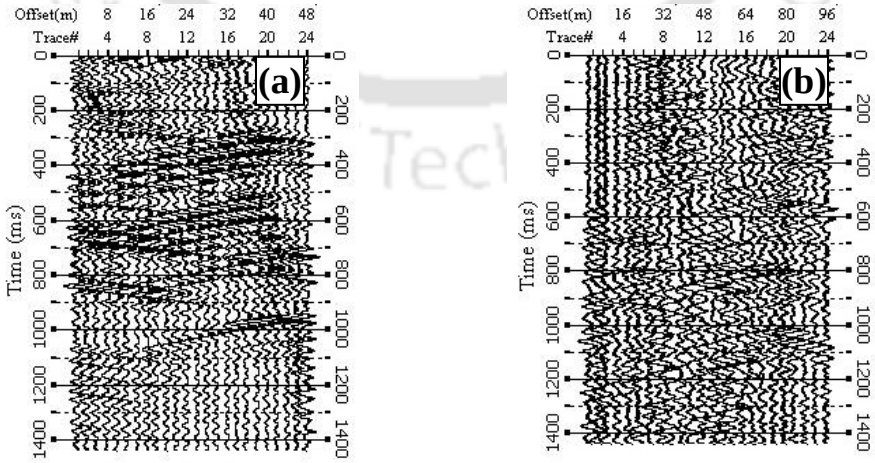

Fig. 25 Field records at Site 3 from (a) 46 m reciever array (b) 92 m reciever array

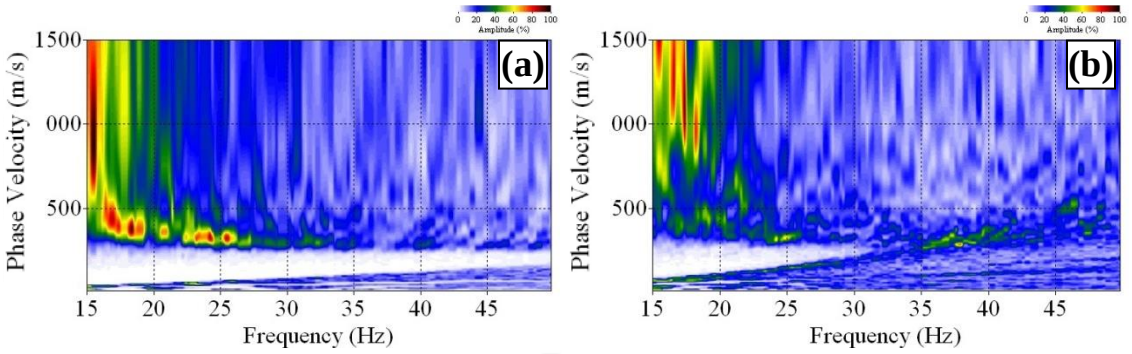

Fig. 26 Dispersion image obtained from (a) 46 m receiver array (b) 92 m receiver array

Validation of the study with active MASW survey (Site 3):

Two typical raw field records collected from the site with an active source of 10 kg sledgehammer have been shown in Fig. 27. The ambience of the site was noisy from incoming traffic generated vibrations and is manifested in the record shown in Fig. 27a. Beyond 16 m offset, i.e. at the 8th receiver position, the active wavefield has been severely contaminated from traffic originated surface waves of large amplitude. With many trials, a comparatively cleaner field record have been obtained as shown in Fig. 27b, which was primarily used for further processing.

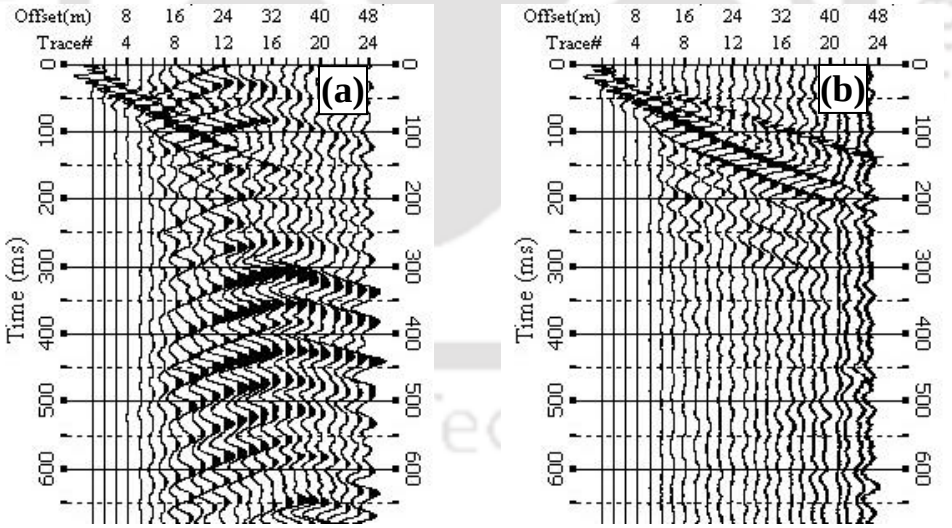

Fig. 27 Raw field record from active survey (a) Active surface event severly contaminated from traffic noise (b) A carefully obtained cleaner record from most possible silent time

In the dispersion image obtained from the cleaner active record (Fig. 28a), the energy trend is similar to that obtained in the dispersion image from roadside survey (Fig. 26a). However, low

frequency band has been observed to have better resolution in case of active dispersion image primarily attributed to the better quality of raw field data and better control in the processing parameters. The selection of dispersion curve on the dispersion image (Fig. 28b) has been restricted within a frequency band of 16 to 31 Hz as energy peaks are indistinct beyond that range.

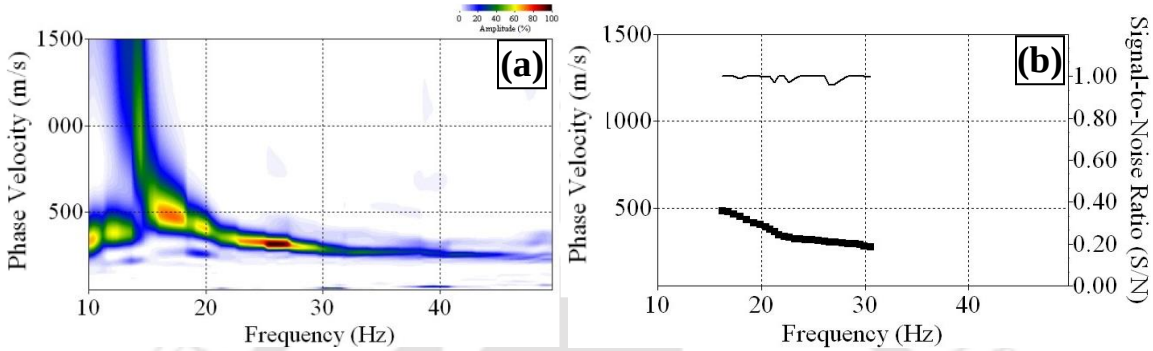

Fig. 28 (a) Dispersion image obtained at Site3 from cleaner active test (b) dispersion curve extracted from dispersion image of active test

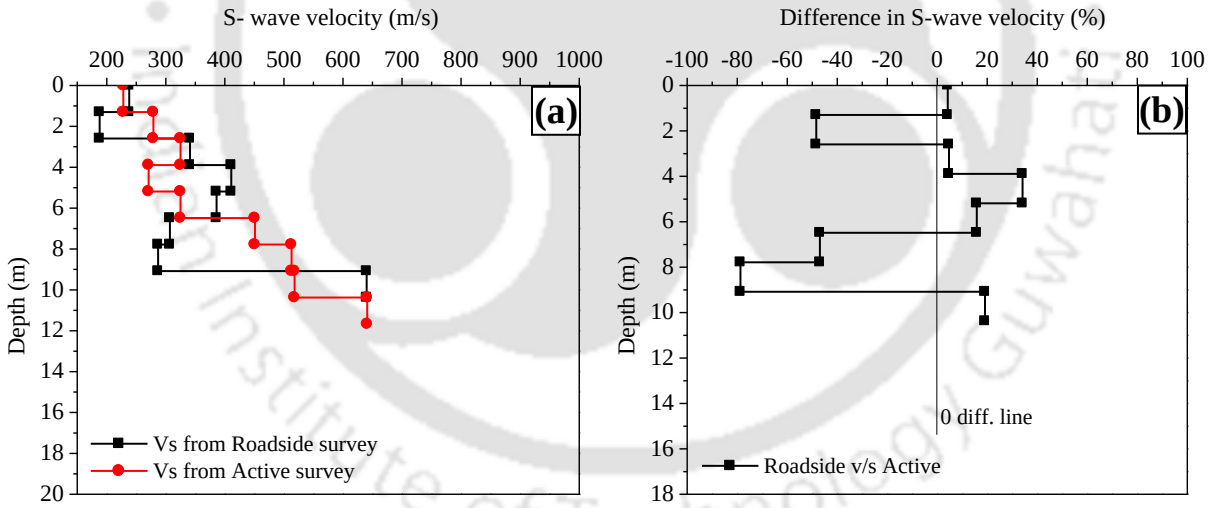

Fig. 29 (a) Comparison of S-wave velocity obtained from passive roadside and active survey at Site 3 (b) Percentage difference of S-wave velocity between passive roadside and active surveys

Shear wave velocity profiles obtained from roadside and active survey have shown some deviations in V_s values in some intermediate layers between 1.5 to 3 m, 4 to 5.5 m, 6.5 to 8 m and 8 to 9 m. From Fig. 29b depicting percentage variation of shear wave velocities between the two profiles, these deviations have been found to be 48 %, 34 %, 46 % and 78 % respectively. These

variations were attributed to the irregular selection of the dispersion curve on some part of the dispersion image from roadside survey that did not have a fully continuous energy band. In other layers, the shear wave velocities well converge to each other. Importantly, the highest wavelength of the wavefield obtained during dispersion curve selection and corresponding depth of investigation from passive roadside survey obtained are 25.9 m and 9.1 m. Therefore, ratio of attainable depth to longest wavelength is 0.35. Similarly, the ratio of longest recorded wavelength to the receiver array length is 0.6.

8.2 Influence of length of Acquisition time

An optimum acquisition time is dependent on the time of occurrence of surface event, distance of origin of the surface wave event from the receiver array and length of receiver array. A shorter array need lesser time and a longer array will require longer time for collecting the surface wave data. The experimentation work intended to decipher the influence of acquisition time has been conducted at Site 2. For the study, eight variations of acquisition times have been adopted as 0.7, 1.4, 2.8, 5.4, 10.8, 21.8, 43.6 and 218 s for testing. Figure 30 and 31 represents dispersion images obtained from the site at different acquisition time with23 and 46 m receiver array. With very limited acquisition time of 0.7 s, dispersion image from 23m array could not exhibit any meaningful information. A shorter receiver array is capable of sampling shorter wavelength or high frequency components of a wavefield. However, high frequency waves propagate slowly through the shallower layers of soil i.e. possesses lower phase velocity. Hence, during a short time span, the high frequency components of the wavefield could not arrive fully to the receiver array and finally resulted in a poor dispersion image. On the other hand, a longer array is capable of sampling longer wavelength or lower frequency components of the wavefield. However, the waves of longer wavelength travels faster through the subsoil, and, hence, reach the receiver array earlier. Thus, in spite of very short acquisition time, some dispersive pattern of waves can be observed on the dispersion image from 46 m receiver array(Fig. 31a), due to the sampling of waves in the lower frequency band (10 to 15 Hz). With a mere increase in the acquisition time to 1.4 s, the dispersion images significantly improved with clearly recognizable dispersive energy band. With further increase in acquisition time (2.8s), the dispersion images becomes a little more distinct (though not significantly), which is attributed to the fact that wavefields from more number of strong sources of wave generation has been recorded in higher acquisition time. It can be identified that

mere increase in acquisition time, e.g. above 21.8 s, does not have much effect on the enhancement of the dispersion image and implies the need of stronger surface event.

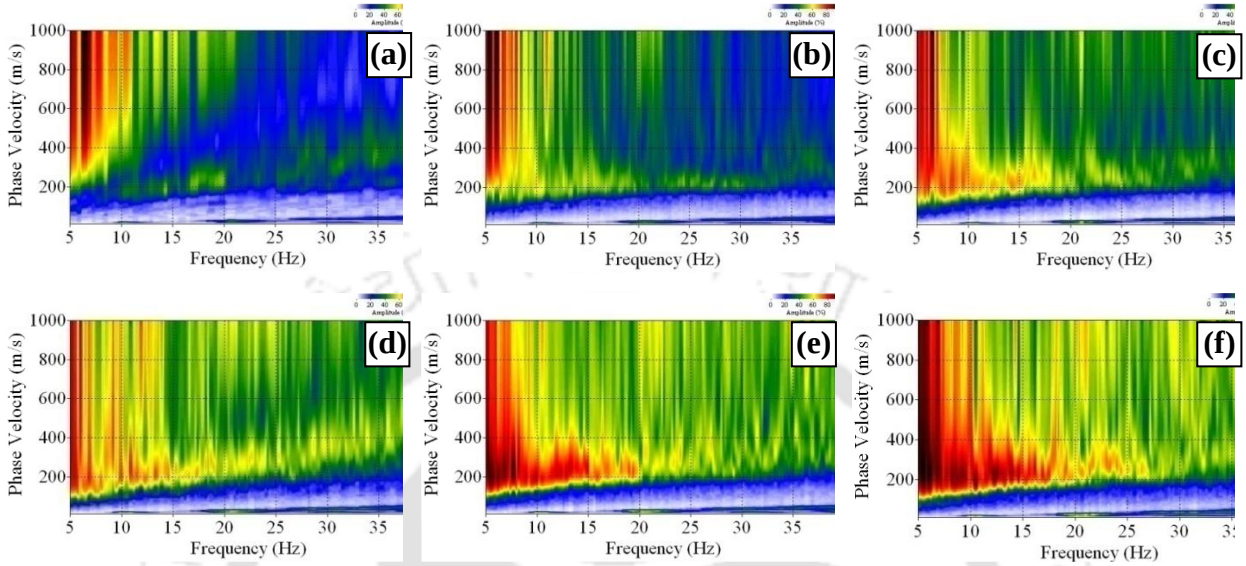

Fig. 30 Dispersion images at Site 1 with 23m array length and with recording time of (a) 0.7 s (b) 1.4 s (c) 2.8 s (d) 10.8 s (e) 43.6 s (f) 218 s

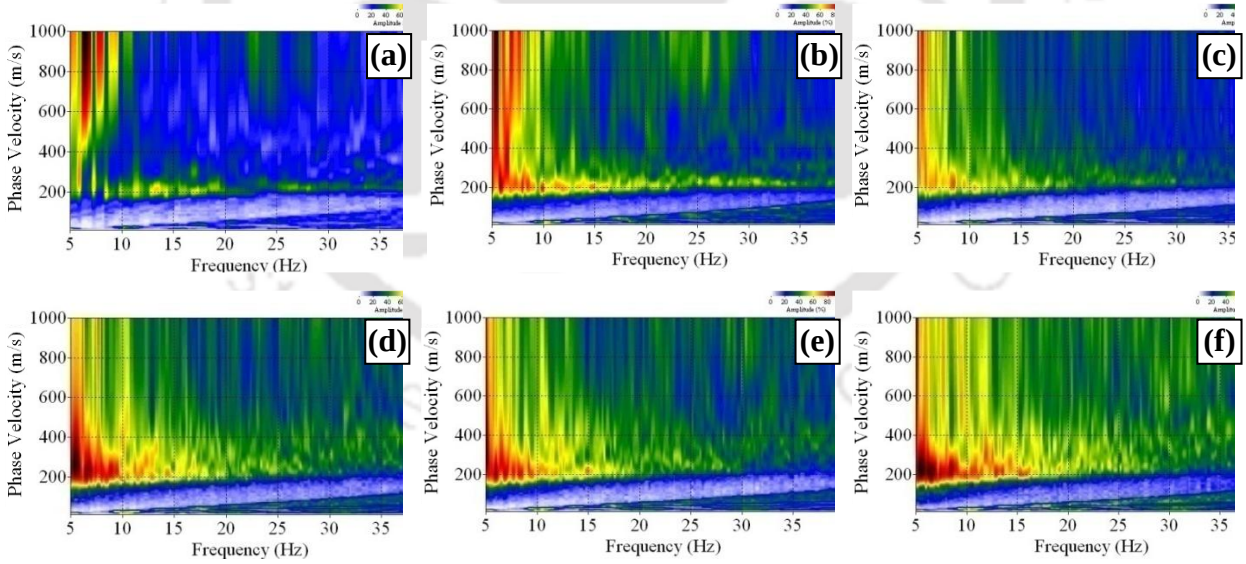

Fig. 31 Dispersion images at Site 1 with 46 m array length and with recording time of (a) 0.7 s (b) 1.4 s (c) 2.8 s (d) 10.8 s (e) 43.6 s (f) 218 s

9. INFLUENCEOF PROCESSING PARAMETERS IN DISPERSION IMAGING

9.1 Optimum selection of frequency and velocity range for dispersion analysis

During dispersion analysis, the first set of processing parameters to be selected are- the optimum scanning ranges of frequency and phase velocity. Every site has its own soil characteristics. At a particular frequency, a site with stiffer soil layers assists the surface wave propagating with a greater phase velocity. Again, surface waves propagate with lower phase velocities at site containing loose soil layers. During dispersion analysis, scanning of true phase velocity is conducted at every frequency component by searching for the greatest amplitude or energy. On the other hand, different sites yield different types of field record with various nature of frequency-amplitude spectrum. Therefore, geologically, the most logical range of scanning frequency and with equivalent phase velocity should be chosen as optimum during dispersion analysis.

Fig. 32a shows a field data from Site 3 processed with frequency and phase velocity ranges of 5-50 Hz and 10-2000 m/s, respectively. It can be observed that the resultant dispersion image lacks the minimum required resolution for dispersion curve extraction. On examining the image carefully, the dispersive wave energy has been identified to be starting from nearly 12 Hz frequency. On reprocessing the record with frequency range of 15-50 Hz and 10-1500 m/s,a dispersion image with high resolution has been obtained (Fig. 32b). Because of higher normalized amplitude at the lower frequency components of the wavefield (<15 Hz), the energy peaks in the other part of the dispersion image in higher frequency band (>15 Hz) have shown relatively lesser energy and sharpness. However, when the frequency band lesser than 15 Hz have been discarded from the analysis (Fig. 32b), the normalized amplitude in the frequency band from 15 to 30 Hz attained their maximum magnitudes and resulted in a dispersion image of better resolution.

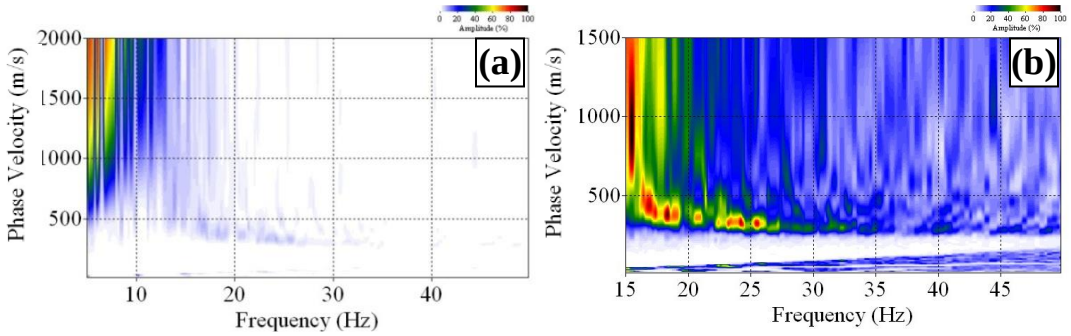

Fig. 32 Dispersion images at Site 3 with scanning range of frequency and phase velocity of (a) 5-50 Hz and 10-2000 m/s (b) 15-50 Hz and 10-1500 m/s

9.2 Optimum selection of Azimuthal range of scanning

In passive roadside survey, as the receiver array is normally placed parallel to the nearby road, at least two quadrants are to be selected to scan all possible incoming directions of the major surface waves from the road (Fig. 33a). However, the selected quadrants may not always cover the major sources of wavefield. In this section, effects of selection of different quadrants during dispersion analysis have been presented. A schematic layout of the position of a major surface source on road with respect to the receiver array has been shown in Fig. 33a. It is evident that all the incoming wavefields from the road surface sources will be arriving at the receiver array from NW-SW quadrants. Dispersion analysis has been performed considering three different quadrants to evaluate the significance of the current aspect. Fig. 33b shows a dispersion image obtained by conducting the analysis considering NE-SE quadrants, i.e. completely ignoring the direction of all possible incoming waves. The computation could not take account of azimuth of any incoming surface waves in the energy estimation and hence no energy peaks are noticeable in the dispersion image. With changing the quadrant to SE-SW, the analysis could partly consider the azimuth of the incoming waves (due to SW quadrant) and energy estimation in the scanning range of phase velocity and frequency range have yielded an improved energy band. As a result, dispersion image of the nature shown in Fig. 33c has been obtained. Fig. 33dshows the best dispersion image obtained when quadrants NW-SW is considered for dispersion analysis. With the aid of Passive Remote Survey, the exact azimuth detection has been performed at Site 1; however, for the sake of brevity, full details are not presented herein.

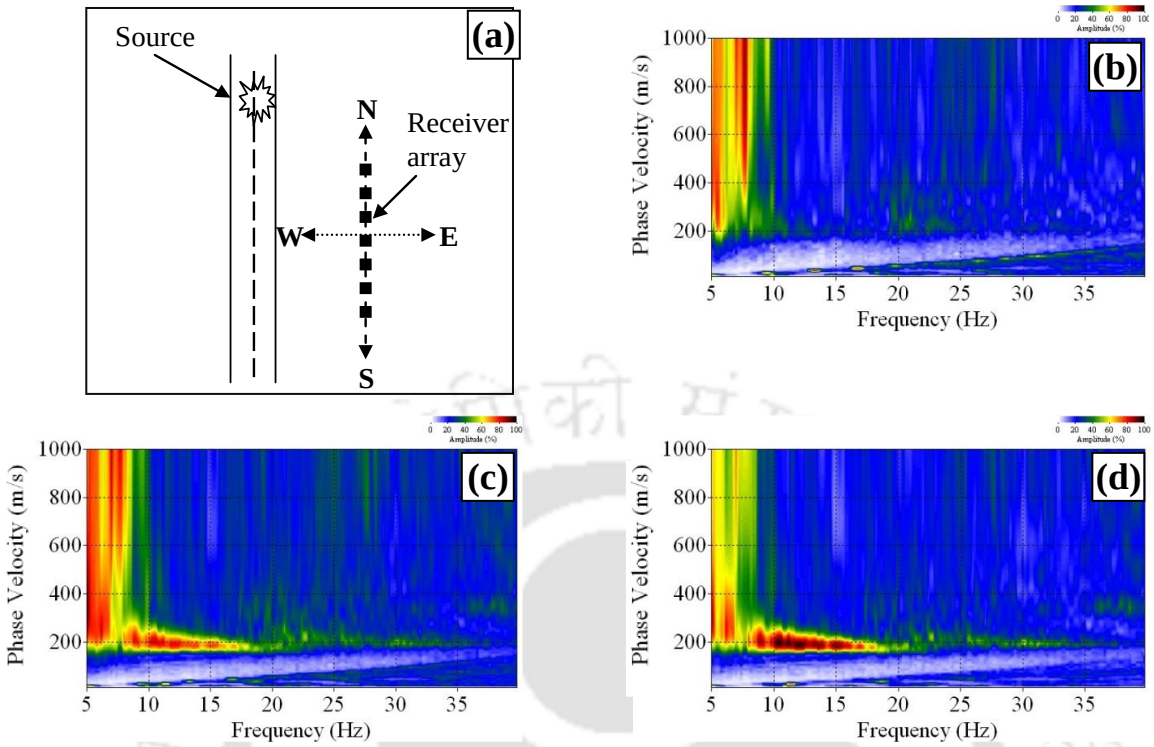

Fig. 33 (a) Schematic of source position with respect to the reciever array. Dispersion images from analysis in quadrant (b) NE-SE (c) SE-SW (d) NW-SW

9.3 Processing with IP, OP and OC scheme

In passive roadside survey, depending upon the positions of the source, wavefield recorded by the receiver array can be of three types- Inline Plane (IP), Offline Plane (OP) and Offline Cylindrical (OC). If a source is situated at a great distance from the receiver array and in-line with the receiver alignment, the wavefield recorded will be of IP type. When wavefields are recorded from a distant source situated not in the same alignment with the receiver array, then the recorded waves can be of OP nature. Further, when a source is situated close to the receiver array and not being in the alignment of the receiver array, then wavefields recorded can be of OC nature. In this section, field data with IP, OP and OC nature has been selected and the comparisons of resultant dispersion images have been presented. Here, three field situations have been selected from Site 1, as shown in Fig. 34. In the first case, field records have been collected when a road surface source was at 20 m offset from the receiver array (IP scheme). In the second case, the records were collected from a source situated within the receiver spread i.e. representing an intra-line source (OC scheme). During both 1st and 2nd case, the offline distance of the receiver array was a mere 5 m from the

center of the road. In the third case, records have been collected from the same intra-line source laying the receiver array at large offline distance of 15 m (OP scheme). It has been observed that when a record collected from the intra-line source with wavefield of OC nature (Fig.34b) was processed with IP scheme, the resultant energy bandwidth of dispersion image is much wider than to the dispersion image processed with OC scheme (Fig.35). As described in Section 8.1.1, a wider energy band in the dispersion image leads to greater possibility of errors in phase velocity estimation. The peaks of the energy band from the OC scheme are much sharper than in case of IP scheme resulting easier extraction of the dispersion curve. In addition, the energy peaks in the lower frequency band have achieved a higher phase velocities in case of IP scheme. However, the dispersion curve extracted from the image of IP scheme has been observed to be in a slightly higher side of the phase velocity range, particularly in the lower frequency band. Similar observations were made when a record collected from the intra-line source with higher offline distance (Fig. 34c) has been processed with IP scheme instead of an OP scheme.

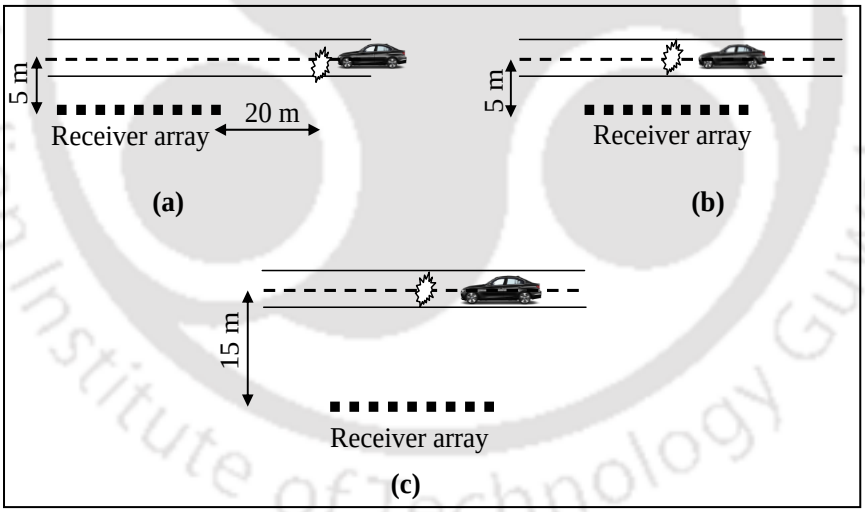

Fig. 34 Three different types of field set up for analysis of raw data simulating (a) IP (b) OC and (c) OP waves

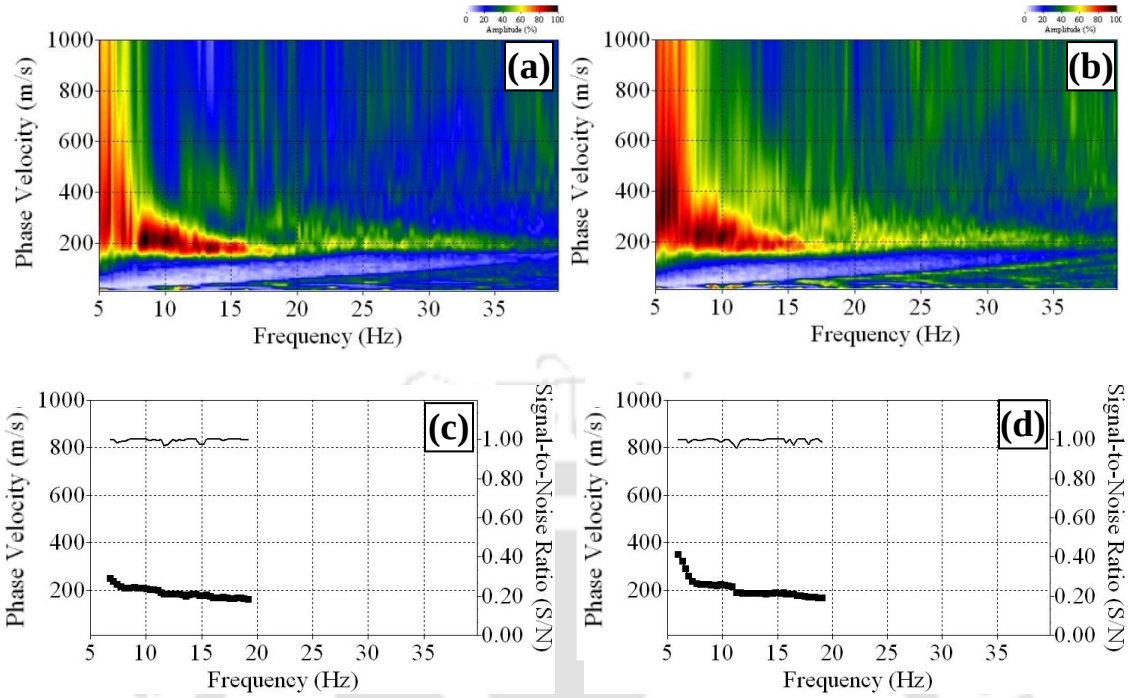

Fig. 35 Dispersion images from an intra-line source at 5m offline distance by (a) OC scheme (b) IP scheme. Extracted dispersion curve based on the (c) OC scheme (d) IP scheme

9.4 Enhancement of resolution of dispersion imaging by vertical stacking

Vertical stacking refers to a technique in which the SNR is enhanced by summing the signals for a number of shots into one set of geophones at one offset (Foti *et al.* 2014). It is also meant for summation of multiple resultant dispersion images obtained from separate field records. A study on effect of different numbers of vertical stacking on the resolution of dispersion imaging for passive roadside survey at the three test sites with different traffic volume has been undertaken. Continuous improvement of dispersion images with increase in the number of stacking (Fig. 36, 37 and 38) have been observed for all the three sites. A single data without vertical stacking could not provide dispersion image of sufficient resolution. The numbers of vertical stacking required for high-resolution dispersion image varies from site to site, depending upon traffic, sources and surface events characteristics. Ten numbers of stacking considering 5.4 s and 10.8 s duration field records have been found to be sufficient for Site 1 and Site 2, respectively; whereas, 20 numbers of stacking of 1.4 s duration field record was found to provide a reliable dispersion image at Site 3.

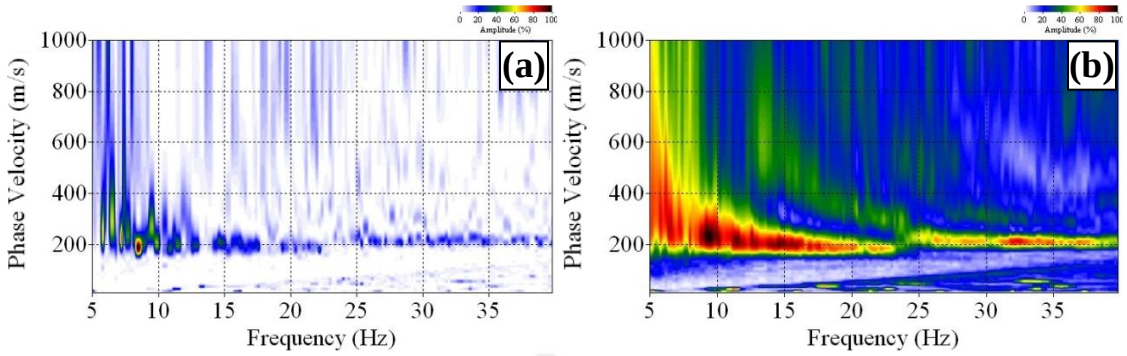

Fig. 36 Dispersion images obtained at Site 1 with vertical stacking (a) No stack (b) 15 stacks

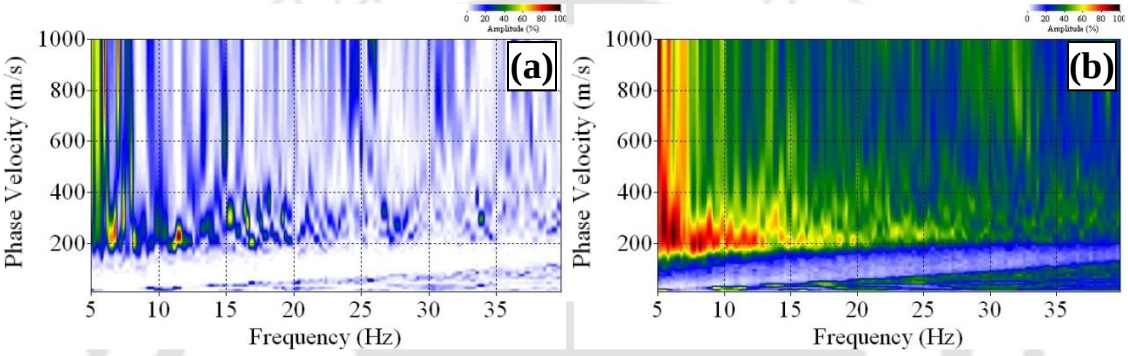

Fig. 37 Dispersion images obtained at Site 2 with vertical stacking (a) No stack (b) 10 stacks

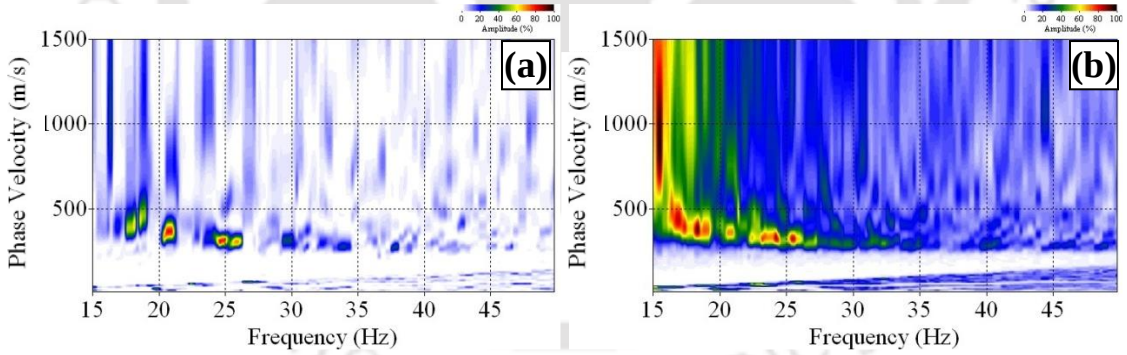

Fig. 38 Dispersion images obtained at Site 3 with vertical stacking (a) No stack (b) 20 stacks

10. OPTIMUM SELECTION OF DISPERSION CURVE FOR RELIABLE INVERSION

10.1 Significance of extracting dispersion points in lower frequency band

The first point selected on the lowest frequency band (longest wavelength) of the dispersion curve determines the maximum investigation depth. In this section, the influence of dispersion points selected from varying lower frequency ranges on the investigation depth and stability of inversion analysis (in terms of RMS error)has been discussed. For the study, a typical dispersion image

obtained from Site 1 has been selected (Fig.39). In the image, four different dispersion curves have been selected, each beginning with a different low frequency dispersion point. The line connecting white dots at bottom represents the selected points of the dispersion curve while black dashed line at the top represent the Signal-to-Noise ratio (SNR) of the selected points. Normally, SNR value close to the value of "1" implies an appropriate selection of dispersion points close to the peak of the spectral maxima. For all the cases of dispersion curve selection from the dispersion image, the SNR value for all the selected points were approximately 1 i.e. the extracted dispersion curve exhibited an overall SNR approximately equal to 100% (with meagre tolerances). In the dispersion curve selections as shown in Fig. 39, the highest frequency bound has been kept constant at 23 Hz and lowest frequency bound has been varied from 12.5 to 5.6 Hz. In Fig. 39a, the selection of dispersion points has been in the range of 12.5-23 Hz. Thereafter, various dispersion curves have been selected considering the lowest frequency selection to be 10 Hz, 7.6 Hz and 5.6 Hz respectively (only 5.6 Hz is shown in Fig. 39b).

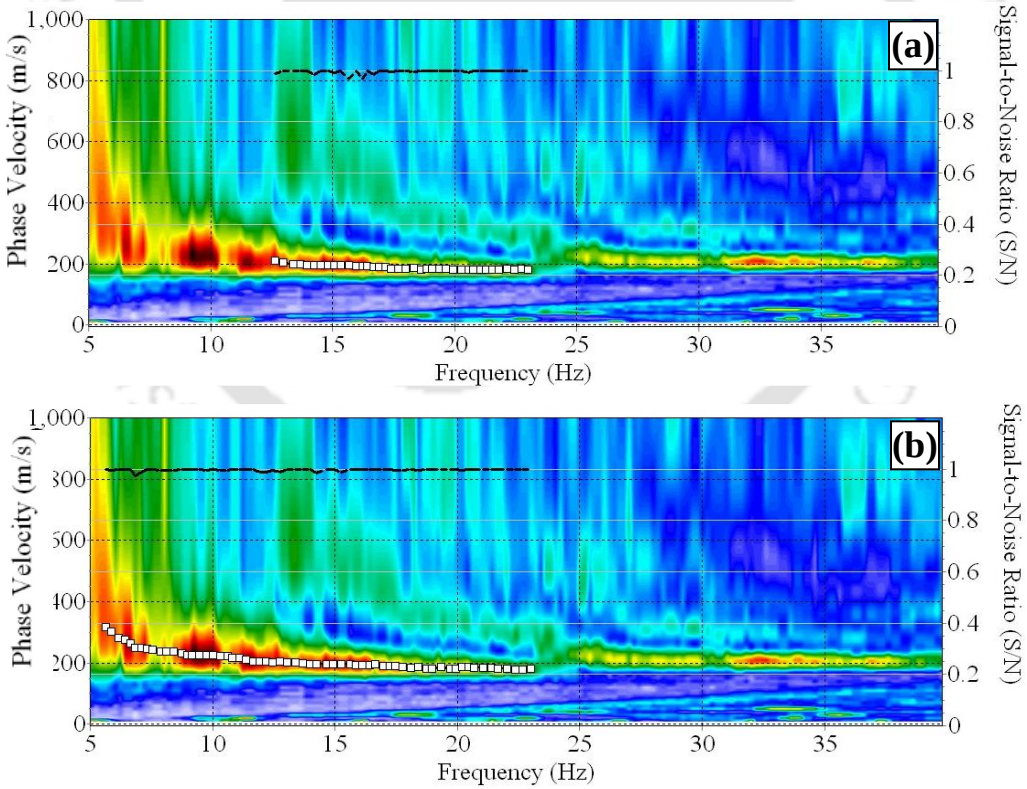

Fig. 39 Dispersion curve selection considering different magnitudes of the lowest frequency (a) 12.5 Hz (b) 5.6 Hz

As observed in Section 8.1.1, different range of selection in the lower frequency band of dispersion curve results in different depth of investigation. Hence, earth layer model of varying numbers of layers ranging from 9 to 14 have been adopted to attain comparable thickness of earth layers in every model. The thickness of earth models were chosen to be of variable nature to incorporate maximum flexibility in the iterations of the inversion process. As the stopping criterion for the inversion, a minimum RMS value of 1.00 and maximum number of iterations of 40 have been selected. Normally, a low RMS value at the end of the iterations implies an appropriate selection of the dispersion curve. Moreover, when a logical dispersion curve (a dispersion curve than cannot be well explained from a theoretical perspective; Xia *et al.* 1999) is processed for inversion, the RMS value drastically reduces during the first few iterations. A prolonged inversion is normally prone to arrive at an impractical V_s profile. Prolonged inversion refers to an unending number of iterations to arrive at a V_s profile. Such occurrence is noticed when the measured dispersion curve trend "does not make sense" from theoretical perspective. This type of dispersion curve normally has an abnormal trend e.g. phase velocity increases with frequency for a significant portion, or the curve flattens at low frequencies. (Surfseis manual, Xia *et al*.1999). Figure 40 depicts the graphical representation of shear-wave velocity variation with depth for different initial frequency bounds applied on the dispersion curves. With selection of 12.5, 10, 6.5 and 5.6 Hz as the lower frequency bound, investigation depth achieved are 5.89, 7.9, 13.4 and 19.7 m respectively. The respective shear-wave velocity profiles converged well to each other with a little deviation at some points.

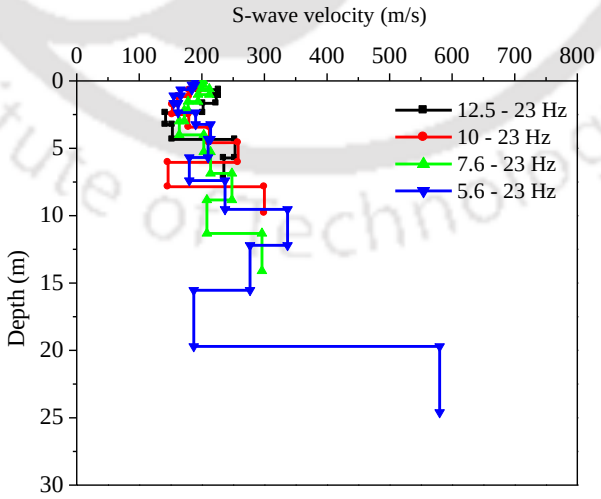

Fig. 40 Shear wave velocity profiles depicting effect of dispersion points chosen from various frequency bands on the depth of investigation

The variation in number of iterations and RMS error due to the changes of the selection in the lower frequency band has been presented in Table 5. The lowest RMS value and highest number of iterations were fixed at 1.00m/s and 40, respectively, as the two stopping criteria of the inversion. With extending the selection of dispersion curve in lower frequency band, RMS values have been found to be increasing. However, the number of iterations required during inversion does not vary linearly with change in frequency range of selection. Based on the trend of increase in the RMS value as observed in this study, it is recommended to restrict the extraction lower frequency range of dispersion curve, depending on the required depth of investigation.

Table 5 Effect of selected frequency range on SNR, number of iterations and RMS value

SL No.	Frequency range of selection	Overall SNR (%)	No. of iteration required during inversion	RMS value in phase velocity after final iteration (m/s)
1	12.5 to 23	99	33	2.12
2	10 to 23	99	34	2.32
3	7.6 to 23	99	9	2.42
4	5.6 to 23	99	21	2.56

10.2 Significance of density of dispersion curve points in V_s profiling

In a dispersion image, the dispersion curve can be constituted by selecting any set of numbers of dispersion points on the energy band. In this section, the effect of number of points, i.e. density of points, of dispersion curves on the final V_s profile has been studied. For this purpose, a typical dispersion image has been selected (Fig. 41) that has been obtained from Site1employing a69 m receiver array. Dispersion curves have been constructed with 5, 10, 15, 20, 30, 40 and 50 number of points (Only two are shown in Fig. 41). All the dispersion curves have been selected within a specific range between 5.5 to 20 Hz, only subjected to the variation of the number of intermediate dispersion points. A SNR value almost equal to 1 has been ascertained in all the cases of selection of dispersion curve.

Figure 42 shows the variation of V_s profiles obtained from processing of the dispersion curves constituted by varying densities of dispersion points. The fluctuations in V_s values among the first three selections i.e. 5, 10 and 15 DC points are much higher than the last three selections i.e. 30,

40 and 50 DC points. The convergence of 30, 40 and 50 DC points and the deviation of other profiles from each other can also be observed in Fig. 42a. Figure 42b shows the variation of V_s profiles expressed in terms of the percentage variation estimated with respect to the V_s profile obtained with 50 DC points. Therefore, for a frequency band of 14.5 Hz (20 Hz - 5.5 Hz), the minimum points required in the dispersion curve for reliable V_s profile has been obtained to be 30. Therefore, it can be stated that for a frequency band of X Hz, the minimum number of points to be selected for the dispersion curve is 2X, i.e. twice of the magnitude of the frequency range under consideration. In other words, the maximum frequency interval between the selections of two points in a dispersion curve should be 0.5 Hz.

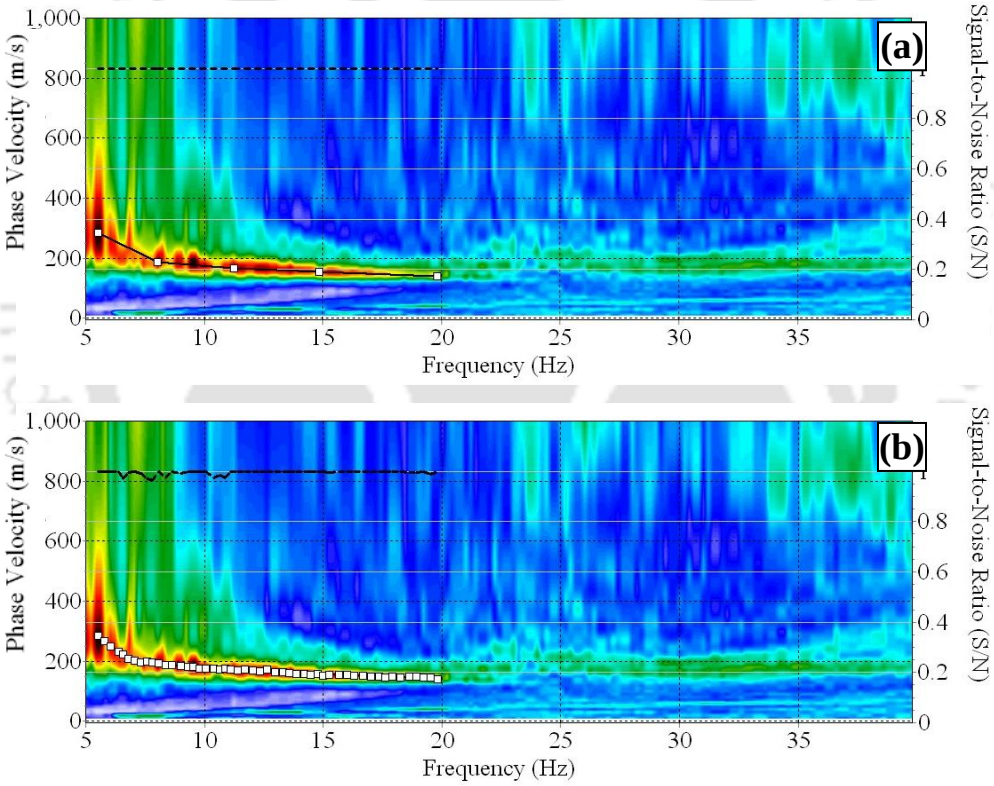

Fig. 41 Extraction of dispersion curve with different numbers of dispersion points from a typical dispersion image (a)5 points and (b) 50 points

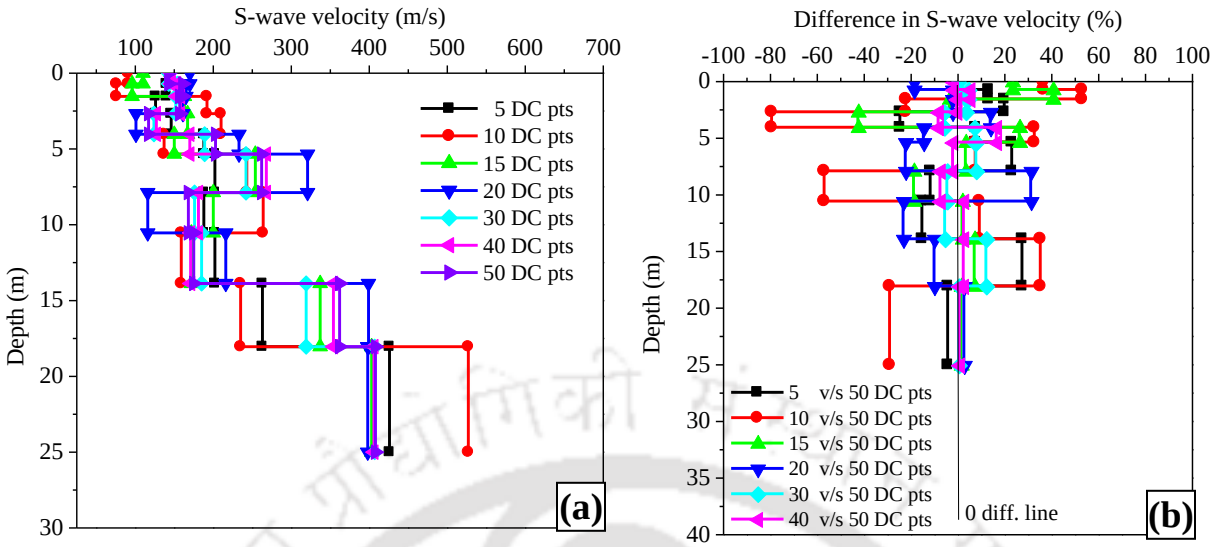

Fig. 42 (a) Variation in shear-wave velocity profile with numbers of extracted dispersion points (b) Percentage variation in S-wave velocity of the profiles with respect to 50 DC point profile

10.3 Effect of initial layer model in V_s profiling

After selection of an appropriate dispersion curve from the dispersion analysis, an initial layered earth model is formed with varying depth, S-wave velocity, P-wave velocity, Poisson's ratio and density. The most efficient initial earth model depends upon the measured dispersion curve. The number of earth strata in a particular depth range is a site-specific parameter and needs a priori information of the geology of the site for appropriate selection. A study has been conducted on effect of varying number of layers in the initial earth model on the final V_s profile and its reliability. A dispersion image and curve has been selected from Site1 with 69 m receiver array (Fig. 41b). The measured dispersion curve has been processed for inversion with varying numbers of layers in the initial earth model in the range of 4-10. The V_s profiles from different earth model have been presented in Fig. 43. It can be observed that the V_s profiles with 7-10 layers earth model well converges to each other. Further, it can be noticed that for lower number of layers in the initial model (less than 5), the obtained velocity profiles deviated from the average trend shown by V_s profiles with 7-10 layer earth model. The deviation of V_s profile obtained from a 4-layer earth model has been found to be highest. Moreover, with decreasing in number of earth layers the approximation in the inversion increases leading to decreasing number of iterations (for those initial earth models having lesser than 7 layers) and increasing value of RMS.

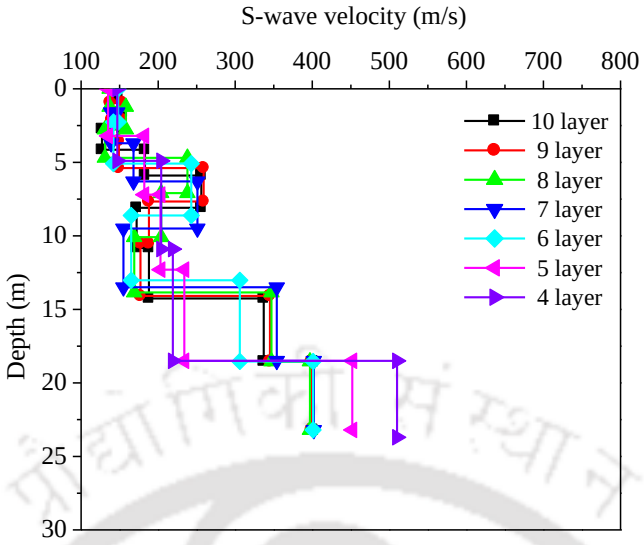

Fig. 43 Shear wave velocity profiles obtained with varying number of layers in the initial earth model

11. SIGNIFICANCE OF SOURCE AND RECEIVER ARRAY POSITIONS IN DISPERSION IMAGING

11.1 Effect of intra-line and outer-line sources

In case of a passive roadside survey, a source position is termed as intra-line (Park and Miller 2008), when it exists within the length of the array. Similarly, in this work, a source has been termed as outer-line when it exists outside the length of the array (Fig. 44). A receiver array can record wavefield of different arrival characteristics such as IP, OP and OC type depending solely on the source positions as mentioned in Sec 9.3. In this section, the effect of intra-line and outer-line source conditions on the raw field record and dispersion imaging of passive roadside data has been analysed for an offline distance of 5 m. The location for all the pilot experimentation has been chosen at Site1.

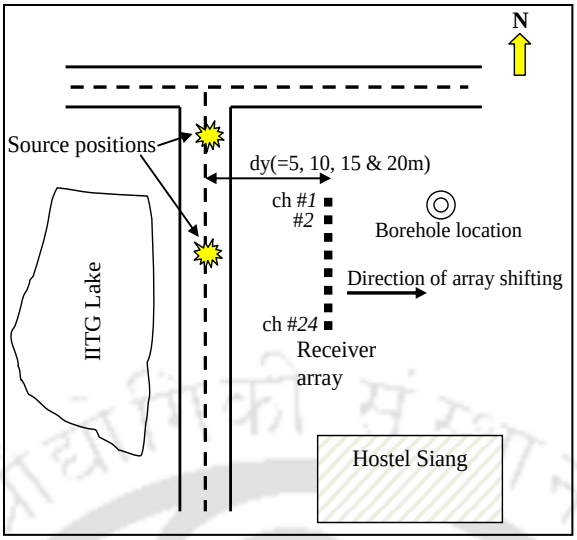

Fig. 44 Schematic layout of different source positions and offline distances in Passive roadside MASW survey at Site 1

Two raw field records with a strong intra-line and outer-line source positions have been acquired during passage of private cars of weight approximately 1000 kg and running at a speed of nearly 30 kmph by the receiver array (Fig. 45a and 45b). It can be observed that there are two prominent wavefields in both the records, manifesting the passing of two vehicles (Vehicle A and Vehicle B) over the source. In the intra-line record (Fig. 45a), the prominent wavefield starts and spreads from a position between 8th and 9threceiver, exactly where the source has been placed on the road. On the other hand, for the outer-line source (Fig. 46b), the raw record has a linear arrival pattern much similar to a conventional active survey. In both the records, a significant blurred portion of wavefield can be observed just below the prominent wavefield (marked as "W" in Fig. 45a and 45b). These wavefields have been created by the two vehicles while moving through the receiver spread after passing the major source. These wavefields are primarily the result of traction interaction of vehicle tires with the bituminous pavement while passing over micro-irregularities present on the road surface, and is recorded owing to their proximity to the receiver array. Careful observations further illustrates that these sources are mostly mini intra-line sources as manifested from their arrival patterns.

The energy band of the dispersion image has been observed to be significantly distinct in the presence of an intra-line source (Fig. 46a). On the contrary, the energy trend in outer-line case

(Fig. 46b) is almost similar as with the intra-line case, although the energy peaks in lower frequency region is relatively indistinct. However, the energy band in outer-line case is relatively thinner which helps in relatively accurate extraction of the dispersion curve. The intra-line source performs better for modal identification in dispersion imaging. The 1st higher order mode (M_1) is relatively more distinct in case of intra-line source compared to the outer-line.

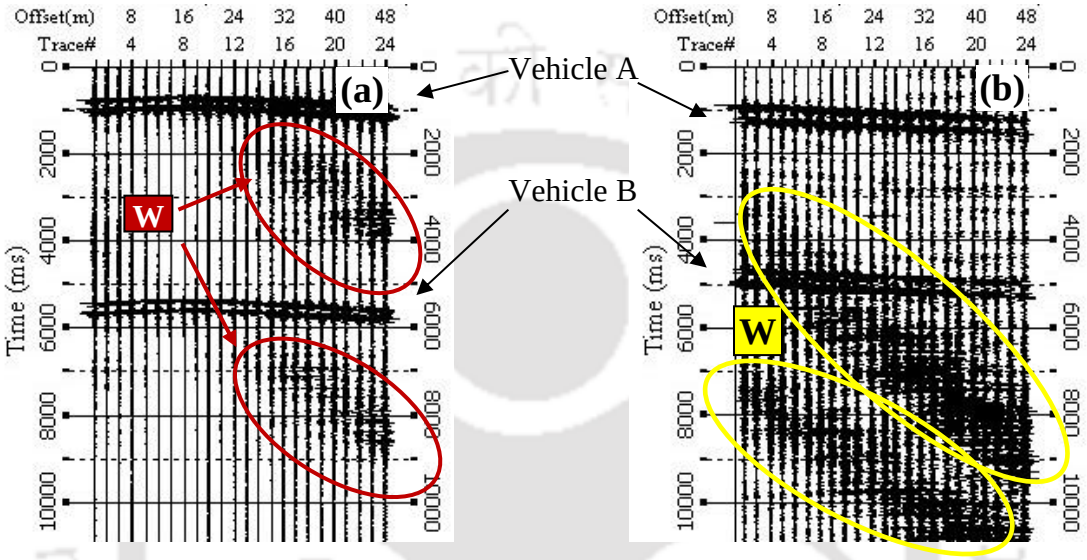

Fig. 45 A typical raw field record with (a) a prominent intra-line source (b) a prominent outer-line source

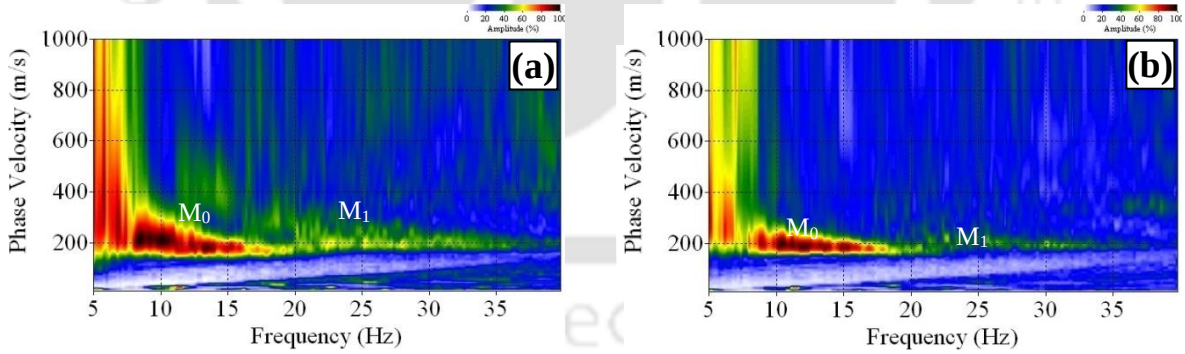

Fig. 46 Typical dispersion images with(a) an intra-line source position (b) an outer-line source position

11.2 Influence of offline distance (*dy*)

In passive roadside survey, the receiver array is to be definitely laid away from the centre-line of the road. A term 'offline distance (*dy*)' is used to denote the distance between centre-line of the

road to the receiver array (Fig. 44). A set of experiments were conducted to study the effect of offline distance on the resolution of dispersion imaging at Site 1. The array was placed at varying offline distances i.e. 5 m, 10 m, 15 m and 20 m from the centre-line of the road, with identical geometrical parameters (Fig. 44). The resolution of dispersion images have been observed to be continually degrading with increasing in offline distance (Fig. 47). The degradation is significant in the lower frequency band. The sharpness of the energy band (which helps in extraction of the dispersion curve) progressively decreases with increasing in offline distance. Moreover, the identification of multimodal characteristics turns out to be difficult with increasing in offline distance.

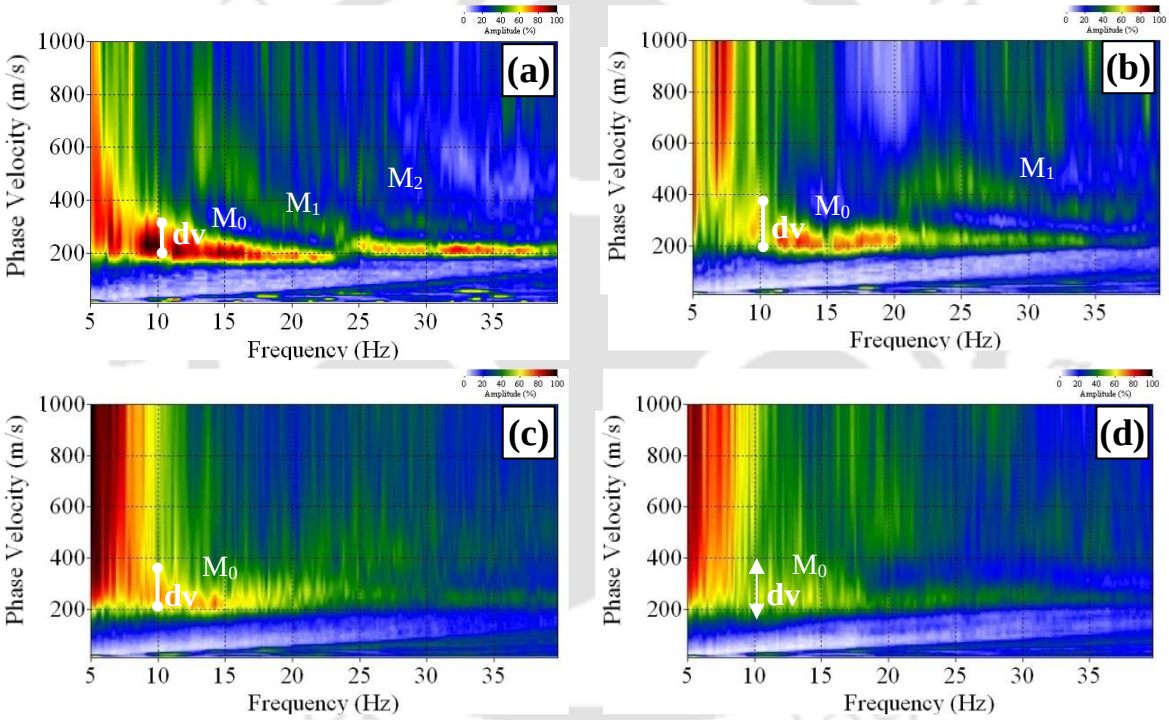

Fig. 47 Dispersion image for varying offline distances (a) 5 m (b) 10 m (c) 15 m (d) 20 m

Resolution of the dispersion image can be defined in a similar manner as in Section 8.1.1with the help of thickness of energy band along velocity axis i.e. *dv*. In Fig. 47, at a frequency of 10 Hz, the value of *dv* are approximately 30, 150, 200 and NR (Not recognizable) at offline distances *dy* = 5, 10, 15 and 20 m, respectively. Therefore, in case of a selection of phase velocity at 10 Hz frequency, maximum possible error is only 30 m/s in case of *dy* = 5m, while for other offline distances the probable error can be of unrealistically higher magnitudes. Such high errors in phase

velocity determination directly affects the accuracy of final shear wave velocity profile of the site, and will eventually lead to a failed survey. Therefore, the largest offline distance that can be used in roadside survey is suggested to be 15 m from the current study.

11.3 Efficacy of Passive Roadside MASW survey

In view of recognizing the reliability and efficacy of the passive roadside MASW survey in generating the resultant shear-wave velocity profiles, the more conventional Active MASW and Passive Remote MASW tests have been conducted and results have been compared. A set of active MASW tests have been conducted at Site 1 for all the different offline distances those were used in the passive roadside tests (Fig. 44) with identical geometrical parameters. Further, a passive remote MASW survey has also been conducted at the site at an offline distance of 20 m utilising mainly traffic originated surface waves. For this study, a circular array has been utilised with a diameter of 18 m. Twenty four geophone receivers were placed along the circumference of the measured array at an inter-receiver spacing (*dx*) of 2.35 m. For a circular array, the inter-receiver spacing is measured along the circumferential periphery of the array.

A borehole test was conducted in the year 2002 near the site of the present investigation. It shows a predominantly loose clayey substratum overlying a stiffer sandy stratum. The Standard Penetration Test (SPT) conducted at the site indicates a low stiffness up to 9 m depth, while it increases thereafter. It is worth mentioning that the location of the MASW test and the SPT test are not exactly in the same place (Fig. 44). Therefore, some differences in the V_s values obtained from the two tests were expected to exist. The receiver location at 20 m offline distance is closest to the location of the borehole survey and hence has been used for the comparison of V_s profile on that particular location. The V_s values from SPT-N values have been obtained by utilising the co-relation ($V_s = 97N^{0.314}$) proposed by Imai and Tonouchi (1982).

At 5 m offline distance (Fig. 48a), both active and passive roadside method gives identical results with close match between the V_s values, the maximum difference being a mere 15%. At locations of higher offline distances, the velocity profile matches closely, except in uppermost 5 m layer where a recognizable deviation occurs between V_s values obtained from the two methods. This difference is mainly due to rapid attenuation property of higher frequency components of passive

surface waves attributed to inefficient recording, leading to missing or misleading information of shallow subsurface layers. Hence, for better resolution in both shallower and deeper layers, an active MASW test in combination with passive roadside test has been carried out. V_s profiles obtained from remote and active survey matches closely with each other (Fig. 48d), exhibiting a mutual reliability. The trend of V_s profile from SPT-N values matches well with the other profiles from MASW surveys, particularly up to 14 m. Beyond this depth, some deviation exists between SPT-N and MASW results, which can be an actual site characteristic, particularly since the sites for MASW and SPT are not exactly the same.

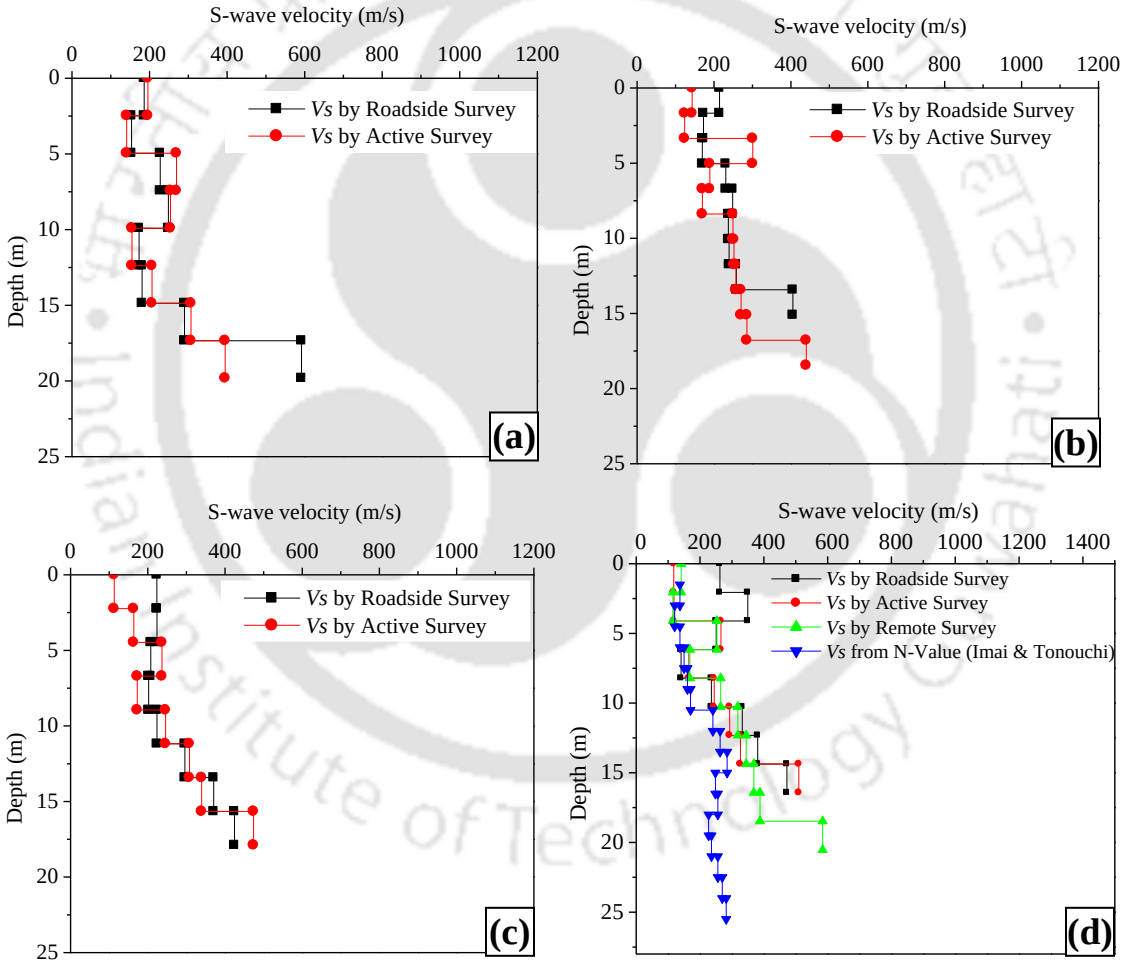

Fig. 48 Shear wave velocity profile at offline distances of (a) 5 m (b) 10 m (c) 15 m (d) 20 m

12. CONCLUSIONS

Based on the various results and responses, the following conclusions can be made on the characteristics of raw field data and resolution of dispersion imaging in case of passive roadside survey.

1. Without presence of major surface sources on the road, traction of any type of vehicle produces significant surface wave energy recordable by the receiver. However, motion of heavier vehicles is more effective for creating wavefield of desired energy for passive roadside survey. Presence of a major surface source has been found to be beneficial for larger impact and generation of higher surface wave energy.

2. Length of receiver array play significant role in the resolution of dispersion image. The ratio between the longest recordable wavelengths to the receiver array length has been found to be in the range of 0.6 to 1. Moreover, the highest ratio between the depths of investigation to the longest wavelength recorded has been observed to be 0.4. In sites with highly noisy environment, longer arrays suffer wavefield contamination, while shorter arrays are effective in sampling dispersive higher frequency components.

3. Acquisition or recording time is completely site-specific parameter and depends largely on volume of the traffic and number of existing sources on the road surface nearby the test site. Smaller recording time is effective during raw data acquisition for thicker traffic flow site.

4. Setting optimum scanning frequency and velocity ranges during dispersion analysis enhances dispersion image resolution by discarding contaminated and/or aliased energy bands.

5. Appropriate selection of azimuthal quadrants allow identifying directions of major wavefield sources making energy computation along azimuth axis constructive and resultant dispersion image with better resolution.

6. An inline-processing scheme for an offline source results broader energy band in the dispersion image, and results in dispersion curve extraction on the higher side of the phase velocities, particularly in the low frequency band.

7. Ten to twenty numbers of vertical stacks is sufficient to develop dispersion images of higher resolution for passive roadside MASW surveys. The number of stacks also depends upon the numbers of raw field records containing major surface event, without which mere increase in number of stacking is not effective.

8. The lowest frequency component on a dispersion curve controls the maximum achievable investigation depth, while on the other hand, increases the RMS errors in the subsurface profile. Depending on the requirement of depth of investigation, selection of dispersion curve should be limited in its lower frequency part to obtain reliable subsurface profile.

9. Density of dispersion curve selection within a frequency range affects the stability of inversion and hence the reliability of obtained shear wave velocity profile.

10. Higher number of layers in the initial earth layer model provides a stable and reliable V_s profile. Lowering the number of layers in the initial model leads to higher deviations in the final profile.

11. Although the intra-line and outer-line source scenarios result in similar energy trends on the dispersion image, a slightly better resolution is obtained in the case of intra-line source is observed in the lower frequency band. The outer-line induced serves a dispersion image with higher resolution in the higher frequency band.

12. Multiple sources have marginal adverse effect on dispersion imaging as long as there is no contamination on the raw records by mutual interferences.

13. The offline distance controls the usability of passive roadside MASW survey. In order to obtain a recognizable dispersion image, the highest offline distance that can be adopted is 15 m from the centerline of the road. Increase in offline distance leads to ambiguous shear-wave velocity profile in the shallower layers within 5 m from the ground surface.

13. RECOMMENDATIONS AND GUIDELINES

Based on the understanding developed from the experimental investigations with passive roadside MASW survey and its analysis, the following recommendations and guidelines have been

developed. Adopting these guidelines during data acquisition and subsequent dispersion and inversion analyses would aid in developing higher resolution dispersion images, leading to reliable estimates of subsurface profile.

- *Guidelines and recommendations for data acquisition*
  - Medium traffic with heavier vehicles (1000 kg or more) with speeds greater than 30 kmph.
  - Simultaneous intra-line and outer-line sources having sufficient spacing to avoid mutual contamination
  - A receiver array length greater than 46 m
  - An acquisition time of 1 s – 10 s.
  - An offline distance less than 15 m from the centreline of the road
  - Adopting minimum 10 numbers of vertical stacks.
- *Guidelines and recommendations for dispersion analysis*
  - Scanning frequency range of 5-50 Hz and scanning velocity range of 10-1500 m/s, with judicious elimination of the low-frequency ranges showing aliasing or banding effects.
  - Appropriate selection of scanning azimuths facing the vehicular movements in the road.
  - Selecting OC scheme for wavefield analysis.
- *Guidelines and recommendations for inversion analysis*
  - Lowest frequency for dispersion curve should be judiciously selected to avoid low-frequency aliasing effect
  - Dispersion point selected should be at every 0.5 Hz frequency
  - Initial earth model with minimum 10 layers should be chosen, or as guided by a-priori borehole survey.

14. FUTURE SCOPES

The following future scopes are identified for further progress of research and understanding in the domain of Passive Roadside MASW survey.

- Further study on the genres of vehicular traffic to establish detailed understanding and guidelines correlating the weight, speed and traction of vehicles passing over different depths of surface irregularities.
- Further studies on various processing schemes such as IP, OP and OC, and strengthening the understanding when the receiver array simultaneously receives various types of waves depending upon the simultaneous location of vehicles.
- Developing automated techniques of dispersion curve extraction to eliminate the subjectivity of the user-based manual extraction.
- Conducting multimodal dispersion analysis.
- Development of robust inversion analysis algorithm.

Relevant References

1. Coccia S, Gaudio DV, Venisti N. and Wasowski J (2010) Application of Refraction Microtremor (ReMi) technique for determination of 1-D shear wave velocity in a landslide area. *Journal of Applied Geophysics* 71:71-89.

2. Comina C, Foti S, Boiero D and Socco LV (2011) Reliability of $V_{S,30}$ evaluation from surface wave tests. Journal of Geotechnical and Geoenvironmental Engineering ASCE 137(6):579-586.

3. Eker AM, Akgün H and Kockar MK (2012) Local site characterization and seismic zonation study by utilizing active and passive surface wave methods: A case study for the northern side of Ankara, Turkey. *Engineering Geology* 151:64-81.

4. Foti S, Lai CG, Rix GJ, and Strobbia C (2014) *Surface Wave Methods for Near-Surface Site Characterization*. CRC press, Boca Raton, Florida, USA.

5. Imai T, and Tonouchi K (1982) Correlation of N-value with S-wave velocity and shear modulus. *Proceedings of the 2nd European Symposium of Penetration Testing*, Amsterdam:67-72.

6. Lin CP, Chang CC and Chang TS (2004) The use of MASW method in the assessment of soil liquefaction potential. *Soil Dynamics and Earthquake Engineering* 24:689-698.

7. Park C.B (2013) MASW for geotechnical site investigation. *The Leading Edge* 32(6):656-662.

8. Park CB and Miller RD (2008) Roadside passive multichannel analysis of surface waves (MASW). *Journal of Environmental and Engineering Geophysics* 13(1):1-11.

9. Park CB, Miller RD, Laflen D, Neb C, Ivanov J, Bennett B, and Huggins R (2004) Imaging dispersion curves of passive surface waves. *74th Annual International Meeting, Society of Exploration Geophysics, Expanded Abstracts*:1357-1360.

10. Park CB, Miller RD and Xia J (1999) Multichannel analysis of surface waves. *Geophysics* 64(3):800-808.

11. Park CB, Miller RD and Xia J (1998) Imaging dispersion curves of surface waves on multi-channel record. *Proceedings of the 68thAnnual International Meeting of the Society of Exploration Geophysicists, Extended Abstracts*:1377-1380.

12. Park CB, Miller RD, Xia J and Ivanov J (2007) Multichannel analysis of surface waves (MASW)- Active and Passive methods. The Leading Edge26:1-6.

13. Stokoe II KH, Wright GW, James AB, and Jose MR (1994) Characterization of geotechnical sites by SASW method. In Woods, RD, Ed., Geophysical characterization of sites: Oxford Publications

14. Xia J, Miller RD, Park CB and Ivanov J (2000) Construction of 2-D vertical shear wave velocity field by the multichannel analysis of surface wave technique. *Symposium on the Application of Geophysics to engineering and Environmental Problems*, Arlington:1197-1206.

15. Xia J, Miller RD, Park CB, Ivanov J, Tian G and Chen C (2004) Utilization of high frequency Rayleigh waves in near-surface geophysics. *The Leading Edge*, 23(8):753-759.

16. Zhang, SX, Chan, LS and Xia, J (2004) The selection of field acquisition parameters for dispersion images from multichannel surface wave data. *Pure and Applied Geophysics* 161:185-201.

List of Publications:

Journals:

1. **Baglari, D.**, Dey, A. and Taipodia, J. "A State-of-the-Art Review of Passive MASW Survey for Subsurface Profiling" *Innovative Infrastructure Solutions*, Vol. 3, Paper No. 66, pp. 1-13 (**DOI: 10.1007/s41062-018-0171-2**)

2. **Baglari, D.**, Dey, A. and Taipodia, J. "Influence of Multiple Source Characteristics and Offline Distance of Receiver Array in Passive Roadside MASW Survey" *Geophysics*. (**Manuscript communicated**)

3. Taipodia, J., Dey, A. and **Baglari, D.** (2018) "Influence of signal preprocessing parameters on the resolution of dispersion image in active MASW survey" *Journal of Geophysics and Engineering*, Vol. 15, No. 4, pp. 1310-1326. (DOI: 10.1088/1742-2140/aaaf4c).

4. Taipodia, J., **Baglari, D.** and Dey, A. (2018) "Recommendations for generating dispersion images of optimal resolution from Active MASW survey" *Innovative Infrastructure Solutions*, Vol. 3, Article 14, pp. 1-19. (DOI: 10.1007/s41062-017-0120-5).

5. Taipodia, J., **Baglari, D.** and Dey, A. (2017) "Resolution of dispersion image obtained from active MASW survey" *Disaster Advances*, Vol. 10(11), pp 34-45.

Conferences:

1. **Baglari, D.**, Taipodia, J. and Dey, A. (2018) "Critical analysis of traffic origin wavefields for optimum utilisation in passive roadside MASW survey" *International Conference on Advances in Concrete, Structural & Geotechnical Engineering (ACSGE - 2018)*, BITS Pilani, India, pp. 1-6.

2. Dey, A., Mukherjee, M., Taipodia, J., **Baglari, D.** and Biswas, S. (2017) "Non-invasive Geophysical Investigation for Subsurface Profiling in Urbanized Megacities" *Extended Abstract: Proceedings of the 2nd Korea-India Joint Geotechnical Workshop*, Seoul, South Korea, pp. 9-10

3. **Baglari, D.**and Dey, A. (2017) "Effects of Source Characteristics in Passive Roadside MASW Survey" *Geotechnics for Natural and Engineered Sustainable Technologies: Indian Geotechnical Conference (GeoNEst: IGC-2017)*, Guwahati, India, pp. 1-4.

4. **Baglari, D.**, Taipodia, J., Biswas, S. and Dey, A. (2015) "Aspects of dispersion imaging scheme of passive MASW survey for subsurface characterisation" *Indian Geotechnical Conference: IGC 2015*, Pune, India, pp. 1-8.

5. Taipodia, J., **Baglari, D.**, Biswas, S. and Dey, A. (2015) "Dispersion analysis using active MASW survey data" *Indian Geotechnical Conference: IGC 2015*, Pune, India, pp. 1-9.

6. Taipodia, J., Budha Ram, B., **Baglari, D.**, Murali Krishna, Dey, A. (2014) "Geophysical investigations for identification of subsurface stratigraphy at IIT Guwahati" *Indian Geotechnical Conference (IGC-2014)*, Kakinada, India, pp. 219-226.